Holocene History of the Lower Seine Estuary and the Commerce Valley Tributary (Normandy, France): A Palaeoenvironmental Framework for the Roman Landscape of Juliobona (Lillebonne) and Implication for Port Conditions

Léa Mairaville, Stoil Chapkanski, Dominique Todisco, Cécile Finco, Christine Paillès, Jonas Parétias, Thierry Lepert, Amine Haddad, Johanne Ducastel, Fabrice Boufflers, et al.

Geoarchaeology

WILEY

Geoarchaeology An International Journal

RESEARCH ARTICLE OPEN ACCESS

Holocene History of the Lower Seine Estuary and the Commerce Valley Tributary (Normandy, France): A Palaeoenvironmental Framework for the Roman Landscape of *Juliobona* (Lillebonne) and Implication for Port Conditions

Léa Mairaville[1] | Stoil Chapkanski[1] | Dominique Todisco[1] | Cécile Finco[2] | Christine Paillès[3] | Jonas Parétias[4] | Thierry Lepert[5] | Amine Haddad[1] | Johanne Ducastel[6] | Fabrice Boufflers[6] | Jérémy Leleu[7] | Laurent Dezileau[8] | Damase Mouralis[1]

[1]Université de Rouen-Normandie, UMR IDEES 6266 CNRS, Mont Saint-Aignan, France | [2]Cerema direction Normandie-Centre, ENDSUM, Le Grand-Quevilly, France | [3]Aix-Marseille Université, CNRS, IRD, Collège de France, INRAE, CEREGE - Europôle de l'Arbois, Aix-en-Provence, France | [4]Caux Seine agglo, UMR 7041 ArScAn équipe GAMMA, UMR 7044 ArcHiMèdE, Lillebonne, France | [5]Université Paris 1 - Panthéon-Sorbonne, UMR Trajectoires 8215 CNRS, Paris, France | [6]Heliadrone, Isneauville, France | [7]Université de Caen-Normandie, UMR 6273 CRAHAM, Caen, France | [8]Université de Caen-Normandie, UMR 6143 M2C, Caen, France

Correspondence: Léa Mairaville (lea.mairaville@univ-rouen.fr)

Received: 12 September 2025 | **Revised:** 4 February 2026 | **Accepted:** 17 February 2026

Scientific Editor: Yijie Zhuang.

Funding: Université de Rouen-Normandie; Caux Seine agglo

Keywords: estuary | geoarchaeology | Holocene | *Juliobona* | palaeoenvironment | Roman period

ABSTRACT

The sediment infill deposits of the Lower Commerce Valley in the Seine estuary, located near the Roman city of *Juliobona* (now Lillebonne, Normandy), provide valuable data on environmental changes during the Holocene, including sea-level changes, sediment supply and anthropogenic influences. A 10-m deep sediment core was collected from the valley deposits, and a multidisciplinary geoarchaeological approach was applied, combining geophysical surveys, dating, sedimentological and diatom analyses. The results reveal a succession of marine to fluvial sediment sequences. At the base, a marine to estuarine environment was identified and then subjected to increasing fluvial contributions. A tipping point is recorded between the fourth and second centuries BCE (ca. 2400–2100 cal. BP) with the establishment of a brackish environment, indicating the progressive disconnection of the valley from marine influences. From the second century BCE, the Lower Commerce Valley appears to have been fluvial-dominated, with no marine influence. This implies that the environment to the south of the Roman city was under freshwater influences. These new geoarchaeological data show no evidence of clogging of the estuarine valley during the Roman period, challenging previous hypotheses linking the decline of the city to the silting up of the valley.

1 | Introduction

An estuary is an interface between sea, river and land, defined by haloclines and tides (Dalrymple et al. 1992). Fluctuating land/sea boundaries (i.e., ecotone, ecocline) make estuaries a challenging geodynamic setting for the reconstitution of palaeoenvironments. Estuaries host a wide variety of environments (marshes, coastal peat bogs, etc.) and provide habitat for

fauna, making this unique combination of territories and resources of strategic interest to humans (Parfitt et al. 2010). In Western Europe, studies of estuaries along the English Channel (Farr et al. 2017) have highlighted various paleoenvironmental successions, coeval with human settlements (Allen et al. 2022; Brown et al. 2010; Havelock 2009; Khan et al. 2015). However, few review articles—even from the past decade—address estuarine adaptations in depth. A three-stage sedimentation model around the English Channel (Long et al. 2000) highlights the role of sediment supply and eustatic control in the silting of southern English estuaries. In France, examples of human relations and adaptation to estuarine changes have been documented in southern Brittany (Baltzer et al. 2015). Understanding past environmental changes to estuaries will enable the Normandy IPCC (Coastal Systems) to refine its projections for, (i) an increase in sea level in Normandy which could reach +1.1 to +1.8 m in Normandy, (ii) the increase in sea level will have an impact on strong winds and storms, (iii) the sediment deficit will exacerbate coastal erosion and marine submersion and (iv) floods will be more frequent and the upwelling of the salt wedge will degrade coastal resources. The palaeoenvironments of the Lower Seine Valley (LSV), a major river in Western Europe (France), have been intensely studied at the beginning of 21st century, and the overall scheme of Holocene sedimentation in the Seine estuary has been described by several authors (Delsinne 2005; Lesueur et al. 2003; Sebag 2002; Sechi-Sapowicz 2012; Sorrel et al. 2009). These studies have been supplemented by investigations focusing on ancient anthropogenic impacts (Frouin 2007; Sebag 2002) as well as more recent ones, particularly since the 19th century (Cuvilliez 2008; Lemoine 2021; Lesueur et al. 2003).

Until now, however, small tributaries of the LSV have remained understudied, contrary to large valleys (e.g., Thames: Khan et al. 2015; Humber: Lamb et al. 2007), probably because the environmental trends in small catchments are not always coeval with the general trends in large catchments (Holliday 1987; Knox 2006).

Several factors make the investigation of smaller catchments' interesting: (i) as they are small, they often exhibit less geological and geomorphological complexity; (ii) due to the local scale, the limited number of environmental variables is suitable for more straightforward monitoring of their interplay and feedback (Notebaert and Verstraeten 2010); and (iii) they are sensitive to external forcings, whether of anthropogenic or climatic origin (Himmelsbach et al. 2015). The theoretical simplicity of these small tributary's catchments may facilitate the establishment of geomorphological models tailored to local conditions (Orth et al. 2004); comparison with other small local catchments is then simplified.

Previous studies aimed at reconstructing the Holocene infilling of the LSV and provided a better understanding of the sedimentary succession. However, the specific palaeoenvironmental changes in the small tributary valleys remain poorly known. The Commerce Valley, situated within the LSV, presents a favourable context to investigate the social and environmental coevolution during the Holocene, with the aim of identifying the controlling factors that may explain the most salient characteristics of the landscape evolution. Lillebonne, formerly called *Juliobona*, was the *civitas*—capital of the Caletes (*civitas Caletorum*), a territory located in the province of *Gallia Belgica*. Researchers presented various hypotheses to explain the social, economic and political changes that affected the city during the third century CE. Among these, environmental determinism (Lespez 2025) suggests that the silting up of the port and the subsequent decrease in commercial activity are key factors. This has been proposed as a possible cause by Duval (1984), Fichet de Clairfontaine et al. (2004) and Spiesser (2021).

The main aim of this geoarchaeological study is to provide a better understanding of the Commerce Valley landscape change, based on both geomorphological and palaeoecological data, specifically to (1) determine the sedimentary dynamics and forcing factors involved in the Holocene filling of the Commerce Valley, (2) propose a diachronous reconstruction of the local environmental succession, by combining sedimentological and bio-indicator proxies, radiocarbon dating and relative sea-level variation data and (3) clarify the geomorphological context during the Roman period.

2 | General Context

2.1 | Geologic Setting

The study area is located in the north-western part of the sedimentary Paris Basin, Normandy region, France. It is mainly composed of a chalk plateau deposited during the Upper Cretaceous (Menillet 1969). Above the plateau lie clays with flints, resulting from weathering of the upper layer of chalk through the Tertiary and Quaternary (Laignel et al. 1998; Quesnel 1997). They are mostly covered by Pleistocene loess with a thickness of several metres (Antoine 2002; Antoine et al. 2021; Meire et al. 2019). The bottom of the dry valleys is often filled with Holocene and/or Pleistocene sediments mobilised by runoff (e.g., colluvium) or solifluction (Meire et al. 2019).

The LSV has undergone major palaeogeographical and environmental changes during the Quaternary, including at least five major fluvial incision phases during the Pleistocene (Genuite et al. 2021, 2025). During the Last Glacial Maximum (LGM), the sea level was about 120 m below the present level. In the Lower Seine estuary, the post-glacial warming resulted in a sea level rise of ca. 25 m since 10 ka (García-Artola et al. 2018; Stéphan and Goslin 2014). Transgressive deposits formed, raising the groundwater table and inducing the development of wetlands and organic sedimentation (Frouin et al. 2009; Sebag 2002; Sechi et al. 2010).

2.2 | Geographic Setting

2.2.1 | *Seine Estuary*

The Seine River watershed covers about 74,250 km^2 of the Paris Basin and flows directly into the English Channel. The mean inter-annual hydrological discharge at the Poses gauging station is about 500 m^3/s, while the maximum of instantaneous discharge may reach > 2000 m^3/s (dataset on hydro.eaufrance: 1990–2006 period). The modern macrotidal Seine estuary is influenced by the English Channel semi-diurnal tides still perceptible as far as the Poses dam, 170 km upstream.

The LSV is commonly divided into three zones: fluvial, middle and marine (Figure 1). The fluvial estuary has a tidal range from a few decimetres at Poses to 3.5 m at Rouen and is characterised by freshwater (GIP Seine-Aval 2013). The middle

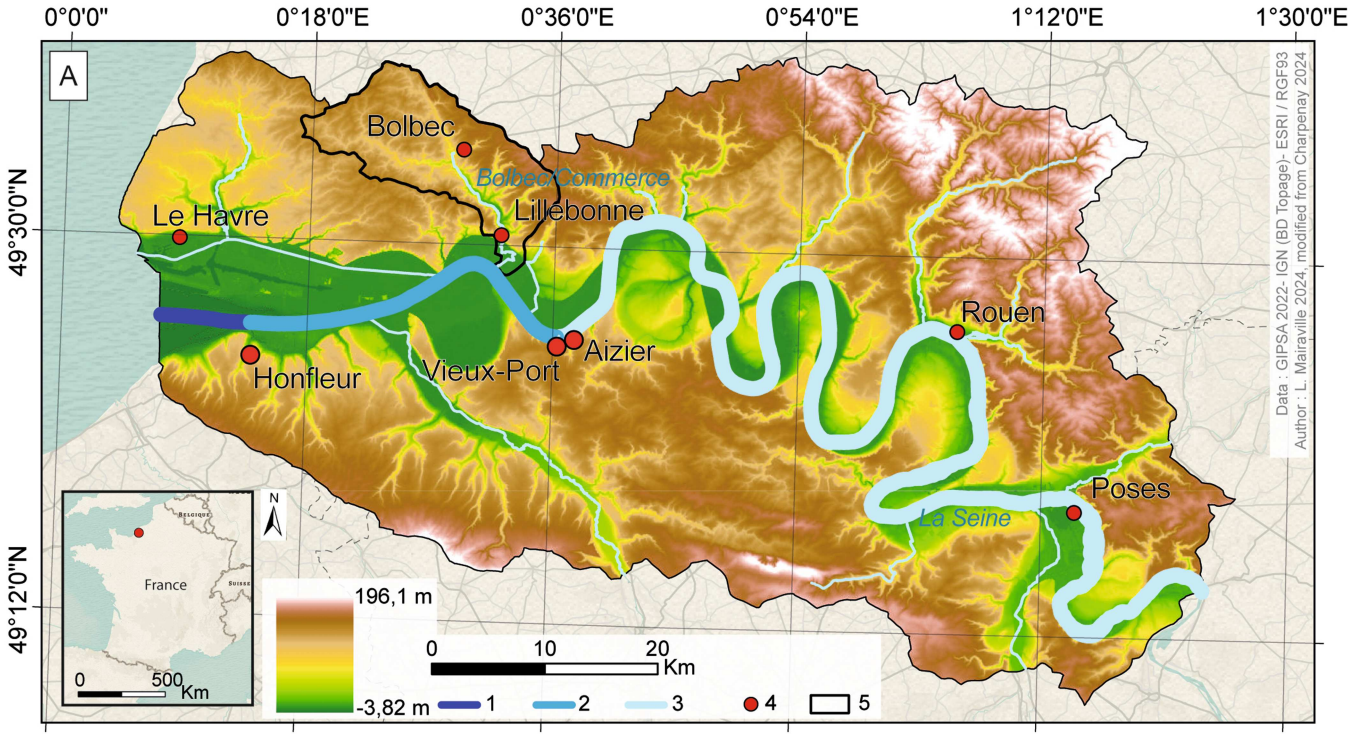

FIGURE 1 | Location of the study area. The Seine estuary: 1: the marine Seine; 2: the brackish Seine; 3: the fluvial Seine; 4: towns on the estuary; 5: topographic catchment area of the Bolbec/Commerce.

estuary has brackish water between Vieux-Port and Honfleur. The marine estuary is influenced by tides ranging up to 8 m at Le Havre with saline water. This segmentation is only applicable for the last centuries due to major damming works on the Seine River that occurred from 1850 (Foussard et al. 2010) and modified these limits (Avoine 1984). These land and fluvial managements modified considerably the local landscape, causing the disappearance of islands, islets and shifting banks, draining mudflats and ancient marshes (Foussard et al. 2010).

2.2.2 | *Lillebonne and Its Watershed*

Lillebonne is situated in the Commerce Valley, which joins the Seine River at the last meander of the LSV's right bank. This meander underwent a succession of right-lateral migrations, now fossilised in the landscape with the presence of a wide floodplain.

The Commerce River is sourced about nineteen km upstream near the city of Bolbec. The mean discharge of the Commerce River over the past 30 years is 0.201 m^3/s, as measured at the Gruchet-le-Valasse gauging station upstream of Lillebonne. In its downstream section, after the city of Lillebonne, the discharge increases by about 0.901 m^3/s. The Commerce River is highly anthropised (Langevin 1998; Jaouen 2019).

The regional climate is temperate oceanic with a mean temperature of 11°C and cumulative daily precipitation ranging between 840 and 1100 mm (MétéoFrance n.d.; Canellas et al. 2014). The watershed of the Commerce Valley is about 176 km^2, covered by 40% grassland and 30% crops, both mainly located on the plateau. Secondary deciduous forests are present mostly on the slopes and occupy about 16% of the watershed (Charpenay 2024).

2.3 | Archaeological Setting

Archaeological evidence suggests that the watershed has been occupied since the Palaeolithic period, yet the Commerce Valley anthropisation increased sharply during Antiquity.

The city of *Juliobona* (Lillebonne) was founded between the end of the first century BCE and the beginning of the first century CE, during the reign of Augustus (27 BCE to 14 CE). The civitas-capital of the *Caletes* reached the peak of its development (about 23 ha based on current knowledge [Parétias 2024]) between the first and the beginning of the third centuries CE. Since 2021, a research programme, entitled '*Juliobona*, *capitale des Calètes*', supported by the local authority Caux Seine agglo, has been providing new data on the configuration of the city, its link with the Seine and human/environment interactions. The location at the intersection of land and river routes provided a favourable context for the maritime activities and therefore the possible establishment of a port (Mouchard 2008).

Even though there is currently no archaeological evidence of the existence of a port in *Juliobona* during the Antiquity (Parétias 2024), this hypothesis persists in local tradition. The argument of a medieval port southward to Lillebonne was used to trace a hypothetical port back to Antiquity (Dubois 2024). However, the definition of a port or a space with port activities must be defined. We can say that (i) a 'harbour' is a natural or constructed space that provides a secure mooring or anchorage (Dictionary Cambridge 2025), while (ii) a 'port' implies more human involvement, with facilities for loading and unloading ships. In the absence of solid evidence and archaeological data to solve this question, it is not possible to certify the existence of a palaeoport or a palaeoharbour at *Juliobona* and in the surrounding area during the Roman period, based on current data.

According to archaeologists (Duval 1984; Fichet de Clairfontaine et al. 2004; Spiesser 2021), the 'decline' of *Juliobona* began in the second century or during the third century CE, although there is evidence of occupation throughout the third and fourth centuries CE. It was hypothesised to be correlated to the decrease of theoretical port activities, possibly due to the sediment infilling of the Lower Commerce Valley and therefore the silting up of the port/harbour. However, the environmental and anthropogenic causes of these changes, as well as the existence and the location of the port/harbour in the valley, remain uncertain.

3 | Materials and Methods

3.1 | Non-Invasive Studies and Core Drilling

A LiDAR-based DTM (Digital Terrain Model) was generated by drone surveys, in order to trace former palaeochannels of the Commerce River. A DJI MATRICE 300 drone was used, with RTK (Real-Time Kinematic) technology to provide highly accurate positioning of each detected point. The drone was equipped with a LiDAR sensor DJI Zenmuse L1 (point rate 480,000 pts/s, horizontal accuracy 10 cm at 50 m, vertical accuracy 5 cm at 50 m), a 3-echo system that reaches the ground through vegetation. The point cloud collected was cleaned and classified, and a DTM was extracted using Pix4D Survey software (v.1.54.1), reaching a mean density of 2500 pts/m^2. It was then analysed using Cloud Compare software (v.2.13.2).

Two complementary geophysical techniques were conducted to determine the location for sediment coring: electromagnetic induction (EMI) and electrical resistivity soundings (ES). These non-invasive methods interpret the responses to electromagnetic or electrical fields transmitted through the ground. The measured properti, the electrical resistivity or its inverse, the electrical conductivity, depends on ground properties, such as lithology, porosity, fluid saturation and salinity (Samouëlian et al. 2005).

EMI provides maps of the spatial variability of electrical conductivity at different depths over the study area. It is well adapted to conductive alluvial environments at the bottom of valleys (Conyers et al. 2008; Verhegge et al. 2017). We used the CMD-Explorer (GF Instruments), in the HCP configuration, covering depths from 2 to 7 m.

ES offers a 1D-view of the subsurface geometry, allowing visualisation of deep interfaces. It was performed with the resistivity-metre Lippman 4-point Light (Geophysical Instruments) using a Wenner-α protocol. The inversion software is IPI2Win.

These two methods helped map the main subsurface interfaces and guided the choice of coring location. The core, C1, ca. 10 m deep, was extracted in plastic tubes using a 1 m-long gouge and a Cobra TTE percussion corer (Atlas Copco) with a hydraulic extractor. The top of the core was located about 4.85 m above the current sea-level NGF (*Nivellement Général de la France*).

3.2 | Chronostratigraphy

The plastic tubes containing the core were opened in the IDEES laboratory UMR 6266, University of Rouen, and the sediments were described, including colour, texture, structure, presence and type of inclusions, any redoximorphic features, porosity and Organic Matter (OM) type. We collected 14 samples for radiocarbon dating (^{14}C) and 15 samples for lead (^{210}Pb) and caesium (^{137}Cs) dating (Supporting Information 1—SI1: Chronostratigraphy). They were all measured in the Radiochronology Laboratory at Laval University (Quebec, Canada).

The raw radiocarbon ages were calibrated using *Chronomodel* software (Lanos Ph. and Dufresne Ph. [2024], see SI1) with the terrestrial northern hemisphere atmospheric calibration curve *Intcal20* (Reimer et al. 2020). All radiocarbon determinations were integrated into an age–depth model, and they were additionally used as Sea Level Index Points (SLIP), integrating previous Holocene sea-level curve reconstruction for French Atlantic and Channel coasts (Stéphan and Goslin 2014).

3.3 | Abiotic Analysis

An integrated approach was developed to investigate core C1: Magnetic susceptibility (MS) was measured along the core, which guided the grain size sampling and geochemical analyses.

Covering stratigraphic diversity as comprehensively as possible along core C1, 41 samples (about 5 g each) were first air-dried and then dry sieved through a 2 mm mesh size for laser granulometry. Thirty-two samples were used to measure carbon [C], hydrogen [H] and nitrogen [N], and 25 samples were subjected to geochemical analysis.

3.3.1 | *Magnetic Susceptibility*

The volume MS (or κ, in $\times 10^{-5}$ SI) was measured with a Bartington Instruments MS2K surface scanning sensor (Bartington Instruments Ltd., United Kingdom) every 2 cm (SI2: Magnetic Susceptibility).

3.3.2 | *Organic Matter Determination and Laser Granulometry*

Carbon [C], hydrogen [H] and nitrogen [N] measurements (in percentage of abundance) were done at the Radiochronology Laboratory at Laval University, with a Leco (CHN628). The organic matter (OM) abundance was converted from carbon [C] measurements using the factor 1.72 (Baize 2021; Pribyl 2010). Prior to grain-size analyses, the organic fraction of the samples was removed using hydrogen peroxide, followed by the addition of a dispersant to prevent clay flocculation. The samples were subsequently analysed using a Mastersizer 2000 laser granulometer (Malvern) covering the grain size range from 2 to 2000 μm. The particle size values (including the median particle size, D50) are calculated for each sample by averaging three replicates taken from the same aliquot. The grain-size pretreatments and analyses were performed in the UMR IDEES - Caen laboratory.

3.3.3 | *Geochemistry and Mineralogy*

Inductively Coupled Plasma-Optical Emission Spectrometry (ICP-OES) was used to determine the quantitative elemental composition of the 25 samples collected along the C1 core. To

avoid uncertainties related to bioturbation, geochemical and mineralogical analyses were not conducted on the first metre of core C1. The sample pre-treatments and measurements were performed in the CRAHAM laboratory UMR 6273 – University of Caen (SI4: Geochemistry and Mineralogy). The concentrations of major elements were duplicated at the *Service d'Analyses des Roches et des Minéraux* from the CRPG laboratory – University of Lorraine, with additional measurements of minor and trace elements. Loss on ignition (LOI) was also determined at the SARM from the UMR CRPG laboratory – University of Lorraine (SI4).

Mid-infrared (MIR) spectroscopic analyses were performed on the same 25-sample dataset, using a Fourier Transform Infrared Frontier Spectrometer, at the analytical platform of Archéorient UMR 5133 – University of Lyon 2 (SI4). Peaks and areas of MIR spectra can be used to estimate the relative abundances of the main mineral groups (tectosilicates, carbonates and phyllosilicates) in coastal sediment deposits (Chapkanski et al. 2022). Specific peak highs and areas of the MIR spectra were then selected to estimate the relative abundance variations of quartz (703–680 cm^{-1}), carbonates (886–868 cm^{-1}), the global clay mineral fraction (929–896 cm^{-1}) and the OM (mostly related to the aliphatic C–H stretch at 3020–2800 cm^{-1}).

The elemental concentrations and the mineral abundances of each sample were merged in the same data matrix. This matrix was used to feed: (i) a correlation diagram (SI5: Correlation Matrix), giving the inter-correlations between the variables and (ii) a principal component analysis (PCA), using PAST (v. 4.03) software (Hammer et al. 2001). These analyses allowed us to (i) decipher the natural clustering of sediments, (ii) explore the down-core sediment variations and (iii) provide insights into their provenance.

3.3.4 | *Mineral, Elemental and Organic Indicators*

Mineral and organic indicators could be used to track changes in sediment provenance and differentiate allochthones from autochthonous sediment contributions. Carbonate materials, quartz grains or zirconium-enriched minerals (Blanchet et al. 2007; Croudace and Rothwell 2015; Rothwell et al. 2006) could be delivered in the lower valley of the Commerce River from both: (i) terrigenous alluvium or colluvium resulting from the weathering of chalky outcrops, the erosion of the Commerce River headwater plateau deposits (i.e., loess; Antoine 2002 or carbonate soils such as rendosols; Baize and Girard 2009) or alluvium from the Seine River headwaters and (ii) marine-sourced sediment transported by the tides along the Seine estuary.

Enrichment of ferric iron, aluminium and rubidium could indicate preferential erosion of clayey materials (Ledieu et al. 2020). These elements are therefore indicative of terrigenous influx associated with clay erosion.

The OM fraction observed in core C1 is presumed to have been formed mainly in situ (i.e., plant decomposition), although a small allochthonous contribution from the local slope erosion of organic horizons cannot totally be ruled out. As no macro-remains of algae nor diatoms were found in the peaty organic sediment (see diatom analysis), we assumed that algae in the C1 core are only a very small contributor to OM.

3.4 | Biotic Analysis

Palynological analyses showed weak preservation with low pollen counts, insufficient to provide a reliable interpretation of past vegetation (Mairaville et al. 2024a, 2024b).

Diatom analyses were carried out at the UMR CEREGE – University of Aix-Marseille laboratory.

Diatoms, *Chrysophycean cysts* (unicellular algae with siliceous tests) and sponge spicules were determined and counted to provide palaeoecological information.

To assess the presence and relative abundance of diatoms, smear slides were prepared using a constant weight of dry sediment and distilled water. Aliquots of the suspension were spread onto cover slips, allowed to dry and then mounted on slides with Naphrax mountant. Approximately half of the 23 samples examined contained no diatoms and were considered sterile. Where diatoms were sufficient, permanent slides of treated sediment were prepared using 0.5 g of dry sediment successively dissolved in hot, concentrated 37% HCl, then in 33% H_2O_2, followed by successive rinsing and decanting with distilled water. Three 200 µL aliquots of the final suspension were deposited on cover slips, allowed to air dry and then mounted on three slides with Naphrax mountant (refraction index = 1.73). These slides were used for diatom counting and taxonomic identification. Counting was performed on two random transects on each slide using a Nikon NS600 microscope at 1000× magnification, with a minimum of 400 individuals counted. In samples with a low diatom content, a minimum of 200 valves was counted in order to obtain ecological information. Diatom concentrations were calculated with the aliquot settling method (Schrader 1974) and expressed in number of individuals per gram of dry sediment.

Diatom identification taxonomic harmonisation followed Lange-Bertalot et al. (2017), Witkowski et al. (2000) and the revised nomenclature in AlgaeBase (Guiry and Guiry 2025).

The fossil diatom flora of the Lillebonne sequence is represented by 97 species distributed among 45 genera. Data are expressed in relative abundance (%). The Shannon diversity index (Shannon and Weaver 1948 in Peet 1974) was calculated and ranged from 0 to 4.6. Equitability, or the equitable distribution of species relative abundances, represents the structuring of assemblages and varies from 0 to 1.

A statistical treatment of the dataset enabled the identification and removal of statistical 'noise' (i.e., species with less than two occurrences and species with less than 1% maximum relative abundance). PCA and Hierarchical Agglomerative Clustering (HAC) (XLStat v. 2012.6.02) were applied to the reduced dataset used to explore the major distribution of diatom taxa and to establish an ecological zonation.

The auto-ecology of each species was compiled from Denys (1991), Vos and De Wolf (1993) and Mertens et al. (2025). In terms of habitat type, species have been classified according to whether they are tychoplanktonic or epontic. Species have also been classified according to their salinity tolerance.

A large proportion of the species in this series are marine, so data on their affinity for nutrients and saprobia in the water are given as 'irrelevant'. However, among the used diatoms, we were still able to propose a classification concerning nutrients and saprobia. About this classification, see SI6: Diatoms Analysis.

The presence of numerous sponge spicules along with diatoms indicates favourable habitat conditions (Łukowiak 2020).

4 | Results

4.1 | Non-Invasive Surveys and Core Drilling

Non-invasive surveys and core drilling were conducted southward of the actual city of Lillebonne (Figure 2A). A topographically lower zone (f) appears to emerge towards the centre of the DTM, but the rectangular edge effects suggest that its interpretation is an artefact linked to acquisition or post-processing. Area (e), which includes plots 84, 26 and 145, corresponds to pastureland that has been grazed and fenced off. At the level of parcel 145, we can also make out a rather vague area (d), slightly lower topographically, without us being able to interpret this further. To the north, on plot 12, several anomalies can be identified: lines (c) and (b) correspond to the paths used by the mowers; rectangle (a) identifies the straight tree plantation dating from March 2023 (Paris-Normandie, 2023-03-10). Despite the quality of the material used and its high resolution, we are not able to distinguish any palaeochannel or other natural traces of the environmental changes.

As revealed by EMI investigations, the study area is subdivided into two main zones (Figure 2B): (i) a conductive zone to the west, exhibiting an apparent conductivity of 40–45 mS/m and (ii) a more resistive zone to the east, in proximity to the Commerce River, displaying an apparent average conductivity of ca. 30 mS/m. The electrical sounding was targeted in the most conductive zones and correlated with the core drilling. It reveals a model of three distinct layers (SI7: Geophysics).

4.2 | Chronostratigraphy and Down-Core Physical Variations

4.2.1 | *Grain Size Variations and Magnetic Susceptibility*

Pictures of the stratigraphic diversity are shown in SI0: Photographs. Since a sediment is composed of clastic elements and OM, we decided to depict it on a single scale (Figure 3). The majority of samples collected along the core are mainly fine-grained with a dominance of clay, silt and fine sands. The MS of sediments along the entire core is relatively low, ranging from -16 to 24×10^{-5} SI. The MS curve displays a majority of negative values, reflecting diamagnetic behaviour, expected for sediments with quartz, feldspars, calcium carbonate, OM or water (Shirzaditabar and Heck 2022), which are the main components of the core C1. We also calculated the sedimentation rates (Figure 4).

The lowest encountered stratigraphic unit (from -10 to -5.77 m below surface level—bsl) consists of homogeneous light grey, greyish silty fine sands (mean median: 35 μm) deposited before 4.5 ka cal. BCE. The sediments are devoid of OM and are deposited in successive laminae. We consider these sediments to be associated with a subtidal flat, also observed by Nanson et al. (2023). They are formed of fine sand with horizontal laminations, without organic content, and they seem to correspond to the tractive sediment filling of tidal channels. The MS shows a sharp decrease around -8 m bsl and then rises again.

This unit is overlaid by organic (> 60%) fine sandy silts ranging from -5.77 to -3.92 m bsl and deposited before 1.6 ka cal. BCE at a mean sedimentation rate of 0.0693 cm/year. The MS values demonstrate a slight increase through the unit, with a median value of about -5 SI. The overall presence of vegetal material suggests a low marsh area upslope of the tidal flat zone (equivalent to '*schorre*' environment of Verger [1995]). Such an area is typically submerged during the highest tides and is covered with halophilic herbaceous vegetation, with a soil made up of fine-grained material, such as mud or muddy sand. The pronounced intermittent emersion allows for vegetation to develop or to be deposited.

The overlaying unit extends from -3.92 to -3.11 m bsl and was deposited before ca. 1 ka cal. BCE. It is made up of grey to brown silty-clay sediments (mean median: 23 μm). The transition of sediments from initially silty-sandy to fine sand and back to silty-sandy (from bottom to top) may indicate a reopening, such as a lateral migration of tidal channels in a tidal flat or low marsh area. The MS values are relatively stable overall (mean: 1 to -5 SI). The only significant magnetic peak is at ~-3.4 m bsl and could be an artefact, as it is not associated with any textural change.

The overlaying stratigraphic unit extends from -3.11 to -2.83 m bsl and consists of fine grey sandy sediment to brown fine silts. The texture of this unit is relatively homogeneous, with a mean of MS values ranging between -1 and -4 SI. These sediments were deposited before ca. 0.9 ka cal. BCE.

The overlaying unit extends from -2.83 to -2 m bsl and consists of organic and clayey-silty sediments. The texture is relatively homogeneous and fine (mean median: 26 μm). The depositional environment exhibits low hydrodynamic conditions, with fine and organic sediments being settled. These sediments were deposited before ca. 0.25 ka cal. BCE.

Based on Figure 4, we also calculated sedimentation rates based on major breaks in the age–depth model: From -3.5 to -2.1 m bsl, the sedimentation rate averaged at ~0.1489 cm/year. The uppermost unit (from -2 m bsl to the surface level) consists of organic-silty with a texture that tends to become finer towards the top. From -2.1 to -1.8 m bsl, the sedimentation rate is around 0.0750 cm/year and increases up to -0.1843 cm/year between -1.8 and -1 m bsl.

4.2.2 | *Relative Sea Level in the Seine Estuary*

The 14 radiocarbon dates that feed the age–depth model (Figure 4) were used as SLIP based on the methodology described in SI3: Sea Level Index Points. They were integrated into a previously established Holocene relative sea level curve of the Seine estuary (Stéphan and Goslin 2014). The linear regression of the C1 core's data (Figure 5A) shows a rate of relative sea level rise of 0.7 ± 1 mm per year between 7 and 1 ka cal. BP/5050–950 cal. BCE. The curve exhibits a high correlation degree ($r = 0.97$), with a determination coefficient (R^2) that explains 94% of the values. These values fit within the trends proposed by Stéphan and Goslin (2014), who indicate a general increase of ≤ 1 mm per year over the last 7–6 ka years. If we only have a look at SLIPs, despite some outliers, our data are consistent with the curve (Figure 5B) proposed by Stéphan and Goslin (2014) and complements the 4–2 ka cal. BP/2050–50 cal. BCE period, where data were lacking.

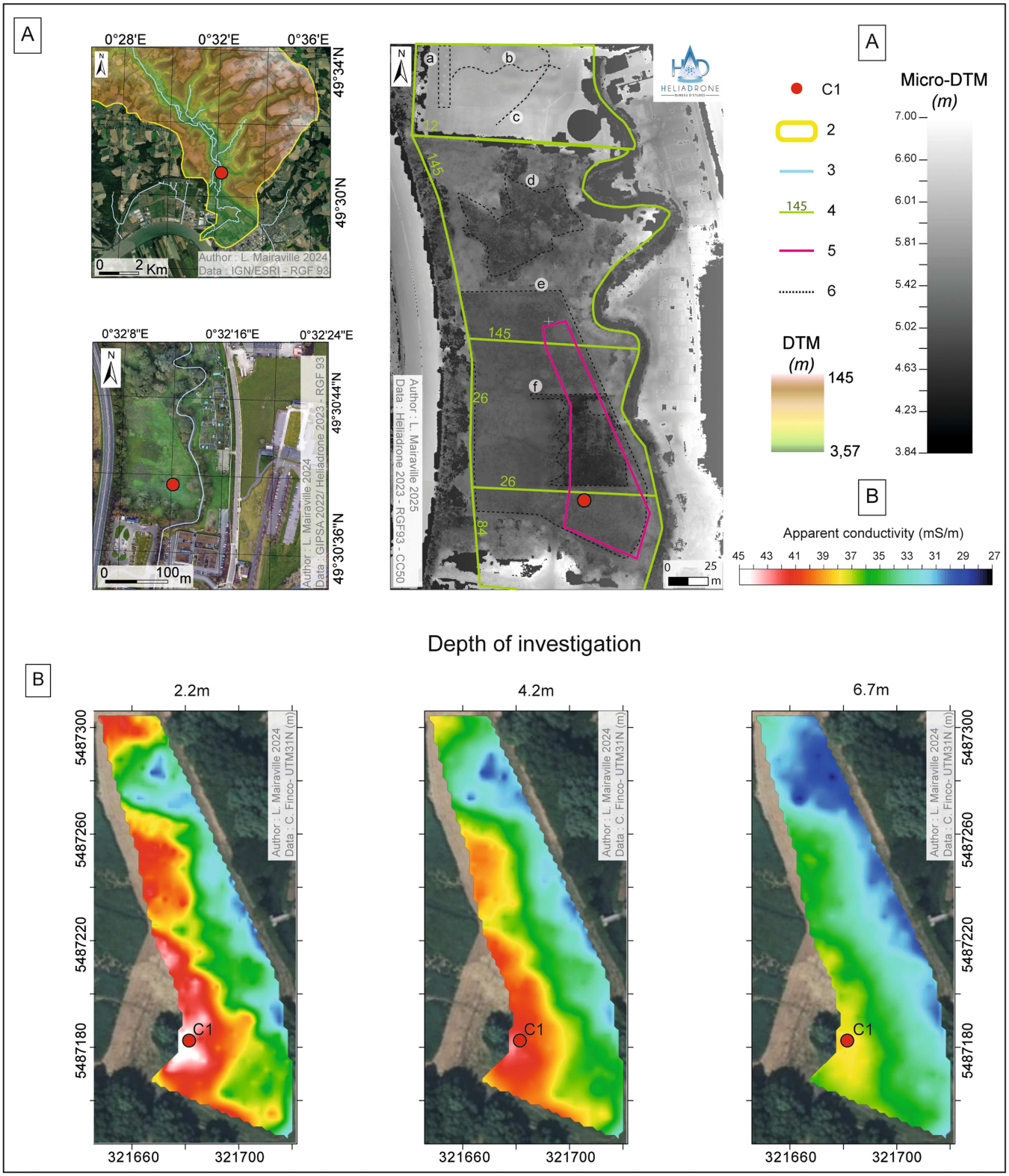

FIGURE 2 | Non-invasive studies. (A) Study location—C1: C1 core; 2: catchment area; 3: hydrographic network; 4: cadastral parcel; 5: geophysical survey; 6: major anomalies from micro-DTM: (a) tree plantation; (b, c) paths; (d) undetermined lower area; (e) pastureland; (f) topographically lower zone, artefact linked to acquisition or post-processing? (B) Apparent electrical conductivity for the three spacings of the CMD-Explorer in HCP configuration.

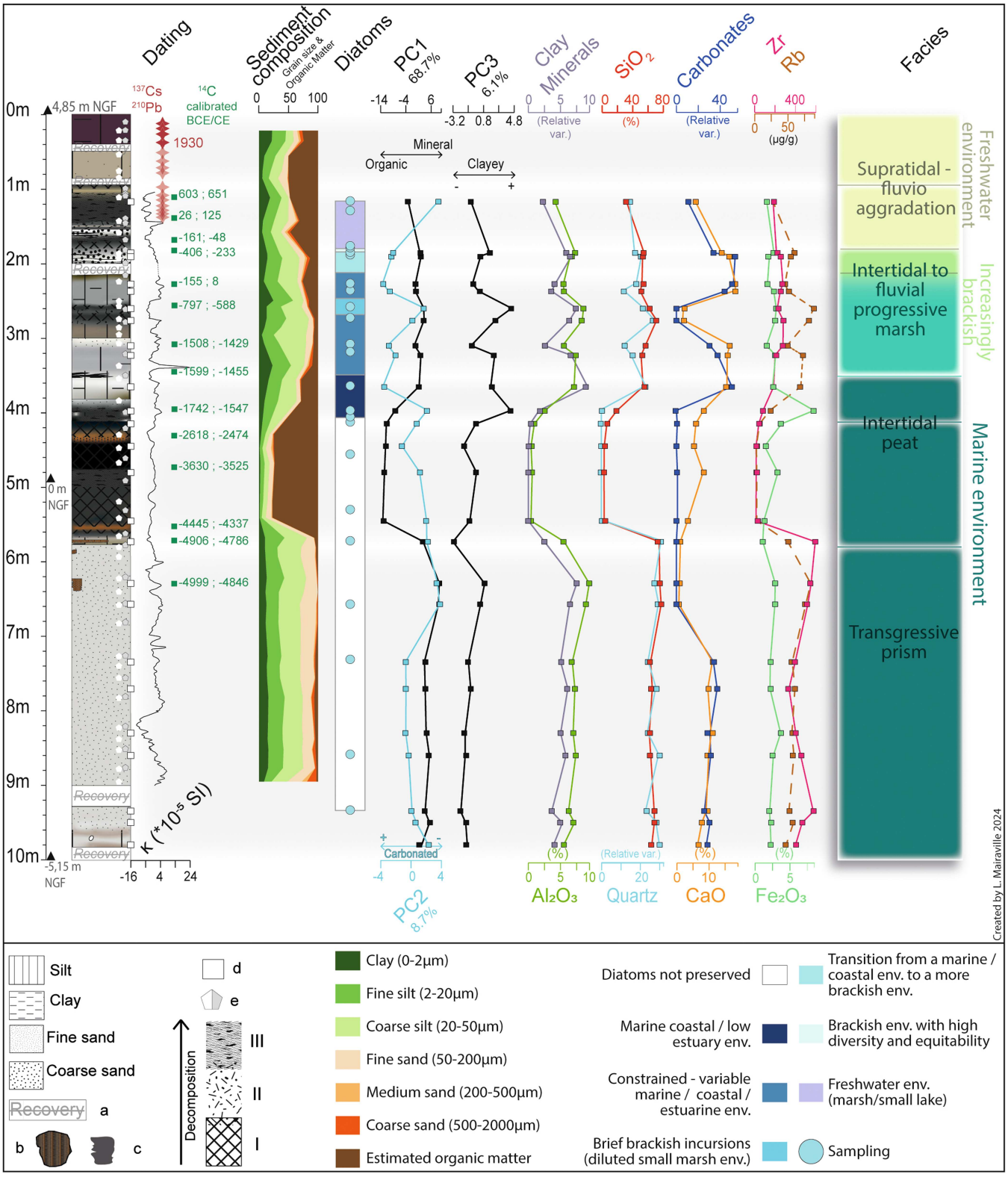

FIGURE 3 | C1 core, analysis and interpretation. Log—a: hiatus; b: organic matter; c: flint; d: geochemistry samples; e: white: grain size sample—grey: CHN sample. I: organic sediment; II: mesic peat; III: sapric peat.

4.3 | Clustering of Sediments and Down-Depth Geochemical and Mineralogical Variations

The most significant geochemical and mineralogical variables (SI5) were plotted against the stratigraphic log (Figure 3).

Figure 6 shows the PCA biplots of scores for the first three principal components, PC1, PC2 and PC3, summarising 85.5% of the total variance. PC1 opposes all organic-rich samples to samples dominated by their mineral fraction, while the second axis (PC2) exhibits the carbonate content of

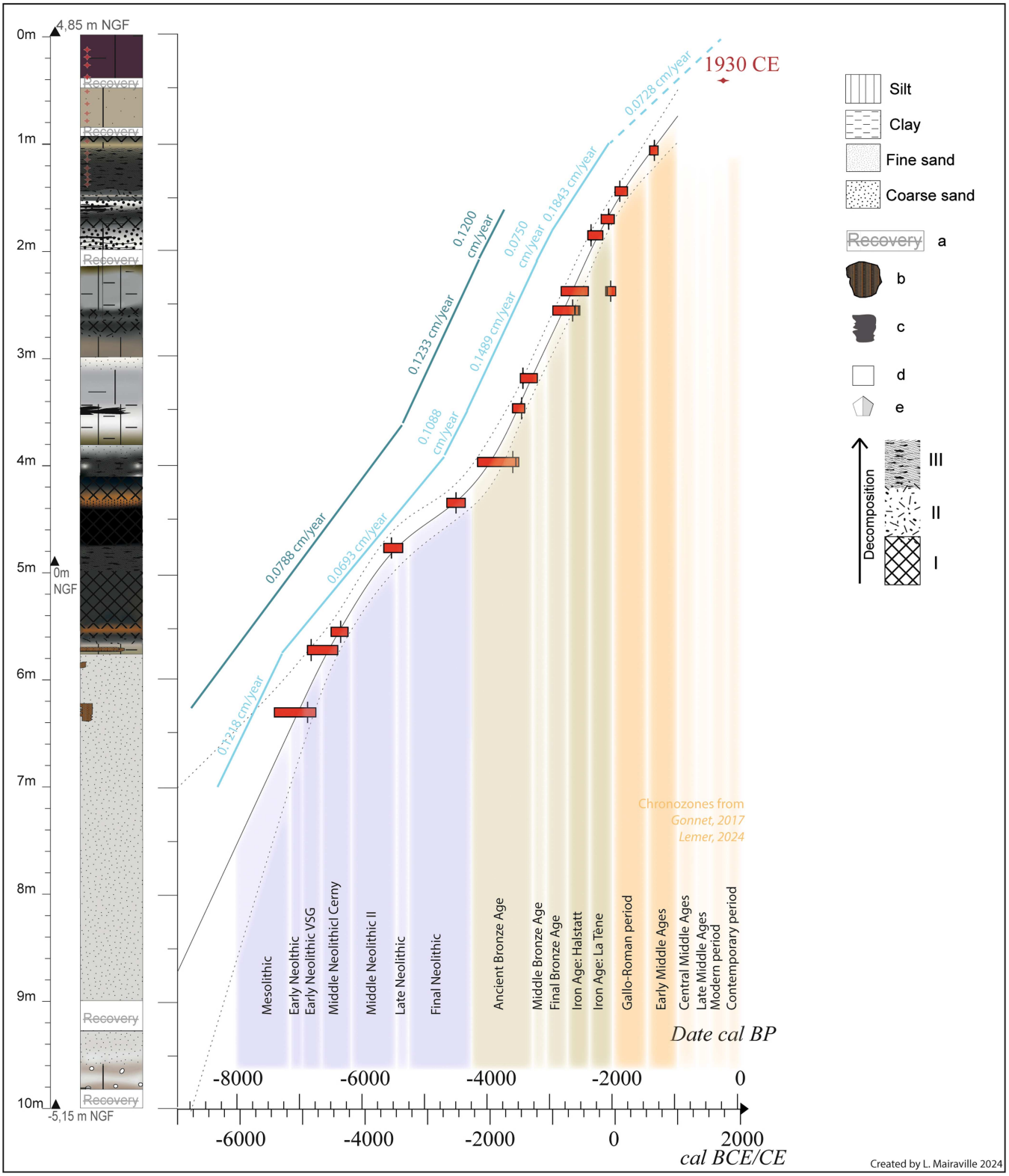

FIGURE 4 | Age–depth model of core C1, developed using Chronomodel software.

sediments (Figure 6A). The PC1/PC3 scatter plot enables a more accurate determination of samples with variable proportions of clay minerals (Figure 6B). These analyses led to the identification of distinctive geochemical and mineralogical patterns of sediments (highlighted in the grey clusters) along the core.

At the base of the core (from −10 to −5.77 m bsl), homogeneous clayey silts and fine sands exhibit relatively high concentrations of Al_2O_3, SiO_2, Zr and Rb coeval with a relatively high abundance of clay minerals and quartz. These sediments also show relatively high concentrations of CaO and Sr, coeval with a significant abundance of carbonates. While carbonate content

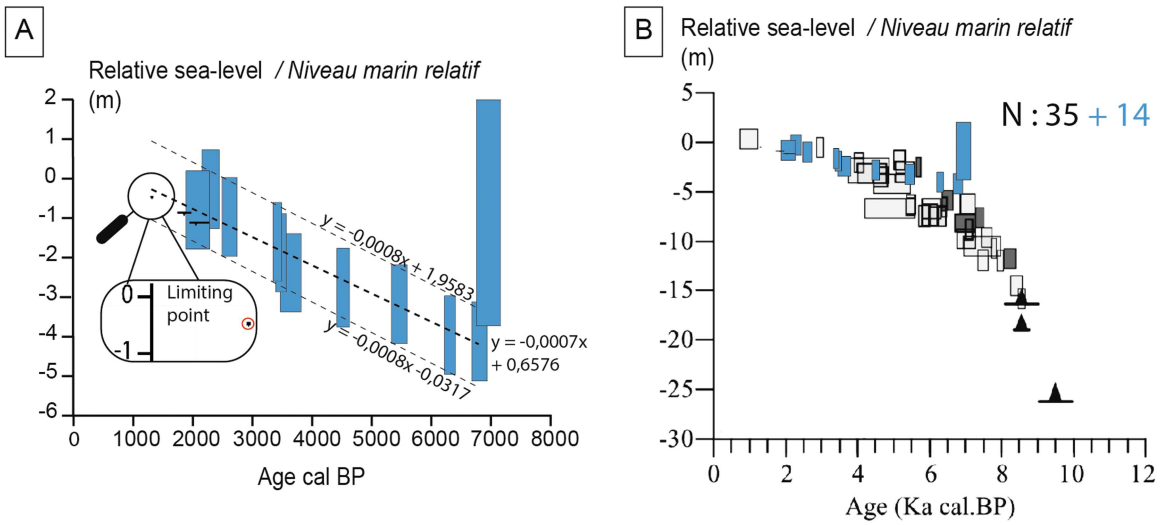

FIGURE 5 | (A) Calculation of SLIPs on core C1 and (B) integration into the Stephan and Goslin 2014 curve.

tends to increase upward (from −10 to −8 m bsl), OM decreases. From −8 to −6 m bsl, carbonate concentrations progressively decrease upward, while clay-mineral and aluminium concentrations tend to increase.

Between −5.77 to −3.92 m bsl, the highest OM content correlates with the lowest values for all the other elemental concentrations and mineral abundances. The sedimentation is presumably mainly autochthonous. The PCA analysis reveals the homogeneity of this unit.

The overlaying unit (from −3.92 to −3.11 m bsl) displays relatively high abundance of silicates, notably clay minerals coeval with Al_2O_3, and quartz coeval with carbonates. These sediments show a low level of Fe_2O_3. SiO_2 and quartz are increasing upward, which could be interpreted as an increasing allochthonous influx.

Between −3.11 and −2.83 m bsl, a decrease in carbonates coincides with an increase of silicates (SiO_2 and quartz + clays). It could be interpreted as an erosional increase of superficial formations in the Commerce watershed.

From −2.83 to −2 m bsl, sediments display relative high abundance of SiO_2 and quartz coeval with clay minerals. At approximately −2.60 m bsl, a decrease in carbonate, CaO and OM abundances reflects a change in the local environment, from a mainly carbonated to a carbonate-devoid siliceous depositional environment.

Stratigraphic analysis reveals that carbonate content reaches its highest levels around 0.6 ka BCE, followed by a gradual decline towards 0.32 ka BCE. At this depth, carbonate contents are coeval with OM but are decorrelated from quartz abundances. This could indicate a greater accumulation of carbonated fractions, possibly derived from close calcareous tuffs found upstream of Bolbec (David et al. 2020). From 2 m bsl until the top, all element concentrations and mineral abundances tend to decrease. Although only three samples cover this upper section, it can be divided into two clusters, with the sample collected at 117 cm bsl, the most recent one, clearly distinguished from all other samples by its highly organic fraction.

4.4 | Biological Indicators (Diatoms)

In the deepest samples examined (between −10 and −4 m bsl), no diatoms were preserved. This could reflect an environment characterised by excessive turbidity/hydrodynamism. The first preserved diatoms appear at −4 m bsl and above (Figure 7).

Zone 9 is identified between −4.10 and −3.50 m bsl. In this zone, the initially low diatom content increased from 0.33 to 1.3×10^7 val/g. The diversity index is 3.7, while equitability is 0.80, suggesting a diverse and well-structured population. Mesohalobic and polyhalobic species are over-represented in this unit, characteristics of a saline to brackish environment. The dominant species are *Paralia sulcata, Thalassiosira oestrupii, Cymatosira belgica, Delphineis minutissima, Raphoneis amphiceros* and *Tryblionella navicularis*, typically from marine, coastal and/or low estuary environments. Numerous fragments of *Thalassionema nizschioides* are present. Planktonic species represent > 65%. Mesotrophic and eutrophic species are also over-represented, reflecting the nutrient-rich nature of Zone 9. Finally, saprobia is also particularly well developed, since the cumulative sum of mesosaprobic and polysaprobic species is ≫ 50%. Sponge spicules are poorly represented (~10%).

From −3.50 to −2.27 m bsl (Zone 10), the marine species from the previous zone developed, while sponge spicules reach ~30%, attesting to a marine/lower estuary environment. The diatom content varied between 0.57 and 1.8×10^7 val/g. However, the lower diversity and equitability compared to the previous unit suggest a more restrictive/variable environment, possibly due to changes in water input (unstable salinity) and/or increased turbidity-saprobia. It could suggest less saline water input in this distal part of the Seine estuary, generating estuarine and variable conditions.

Indeed, this marine episode is interrupted at ~−2.60 m bsl (~−860 cal. BCE/1090 cal. BP) by a sudden decline (Zone 11) in marine species while species tolerant to variations in salinity (oligohalobes + oligohalobes-halophiles) such as *Nanofrustulum sopotense*, *Pseudostaurosira elliptica*, *Pseudostaurosira subsalina* and *Staurosira venter* proliferate. This episode also corresponds to the development of eutrophic and mesosaprobic species. This change might reflect a more diluted (less saline)

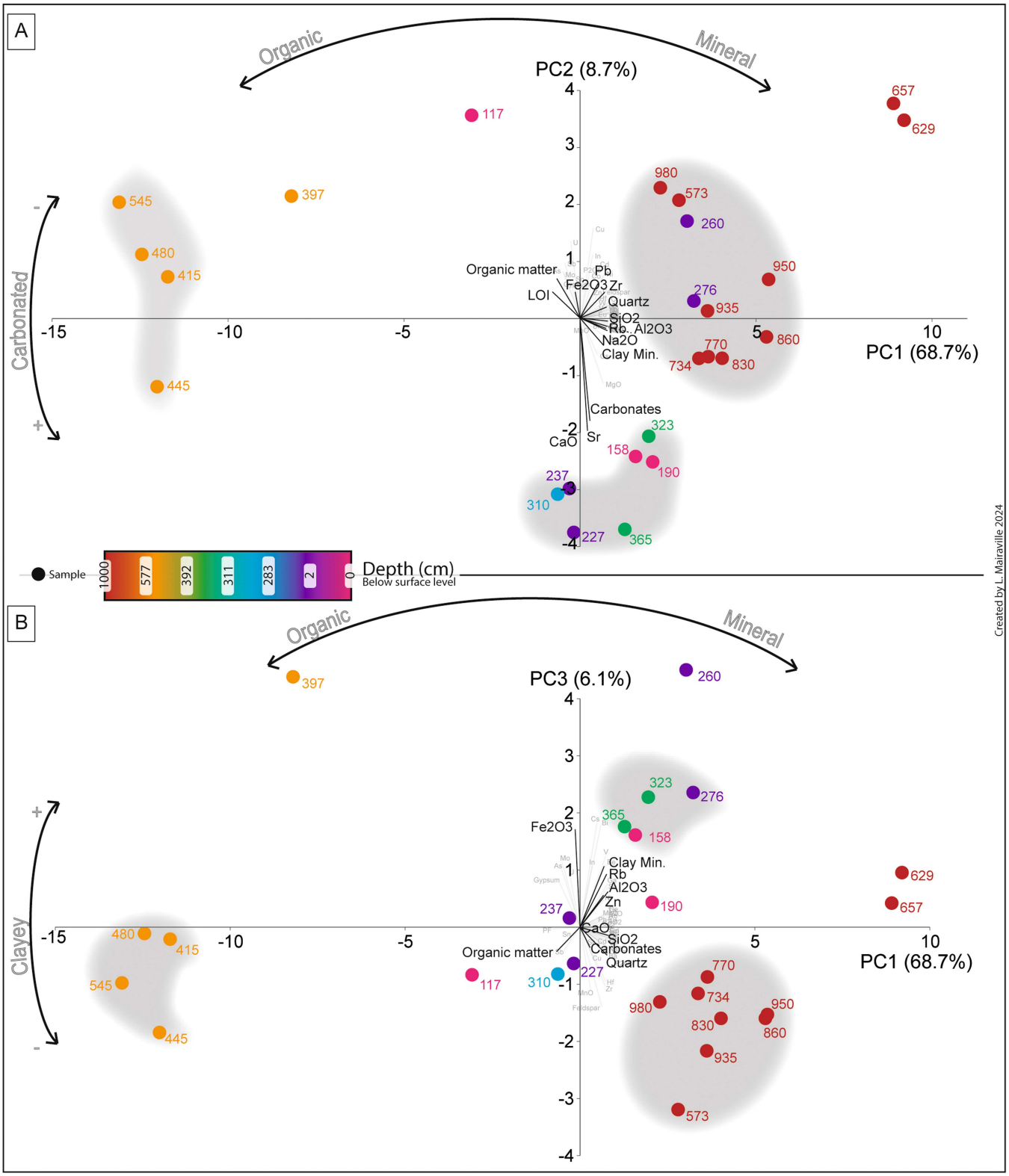

FIGURE 6 | Principal component analyses of mineralogical and geochemical analyses of core C1. A: PCA n°1, PC1 vs PC2. B: PCA n°2, PC1 vs PC3.

environment, as supported by the punctual occurrence of *Chrysophycea cysts* (10%).

From ~−1.85/90 m bsl, in Zone 12, the polyhalobic species progressively decline and disappear in favour of species tolerant to salinity variations, such as *N. sopotense*, *P. elliptica*, *P. subsalina* and *S. venter*. Mesotrophic and mesosaprobic species skyrocket, showing a more and more diluted (brackish) environment as supported by the increasing occurrence of *Chrysophycea cysts* (from 0% to ~4%).

In Zone 13, a gradual development of freshwater species (*Aulacoseira italica*, *Cocconeis placentula*, *Epithemia turgida*, *Ulnaria capitata* and *Ulnaria ulna*) is observed. It is correlated

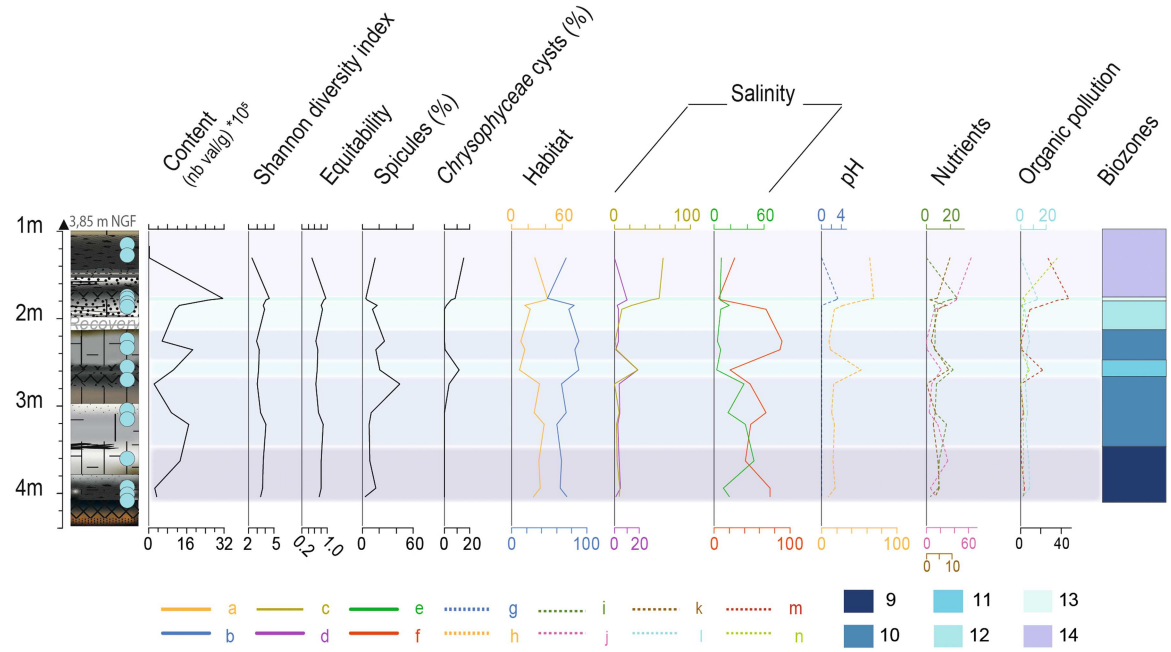

FIGURE 7 | Variations in habitat, salinity, pH, nutrients and organic pollution in diatoms through core C1. Results of diatom analysis on core C1. a: epontic; b: tychoplanctonic; c: oligohalophilic; d: oligohalophilic–halophilic; e: mesohalophilic; f: polyhalophilic; g: acidophilic; h: alkaliphilic; i: eutrophilic; j: mesotrophic; k: oligotrophic; l: polysaprobe; m: mesosaprobe; n: oligosaprobe. 9: marine and coastal/low estuary environment; 10: restrictive-variable marine/coastal/estuarine environment; 11: brief brackish incursions (diluted small marsh—brackish environment); 12: transition from a marine/coastal environment to a more brackish environment; 13: brackish environment with high diversity and equitability; 14: freshwater environment (marsh/small lake).

with a decrease in tychoplanktonic species and a punctual increase of eutrophic and polysaprobic species, supporting the idea of environmental disruption, with a probable input of nutrients and OM from freshwater.

Above −1.77 m bsl, brackish water diatoms decrease, while freshwater diatoms (*Pinnularia* spp. and *Gomphonema* spp.) and *Chrysophycean cysts* (*reaching 15%*) develop and indicate a freshwater pond/swamp disconnected from the marine/coastal environment (Zone 14). The development of meso-eutrophic and meso-polysaprobic species could suggest the increased nutrient inputs from human origin. Above this zone, diatoms are absent.

5 | Discussion

The Holocene palaeoenvironments identified through the study of the Commerce Valley infill can be discussed to estimate if they were favourable to the establishment of a port near the city of *Juliobona*, during the Roman period.

5.1 | Depositional Environments

The multiproxy data enable the reflexion upon Holocene depositional environments in the downstream part of the Commerce Valley. A schematic extrapolation is provided to facilitate the understanding of the local environmental changes (Figure 8).

The basal recorded facies took place before the second millennium (mlm) BCE (ca. 3.6 ka cal. BP) and could be subdivided into three sub-marine facies.

The lowest facies is developed before the fifth millennium (mlm) BCE (ca. 7 ka cal. BP) and corresponds to a relatively tractive outer estuarine sedimentary environment characterised by a mixed (sandy/muddy) floodplain with high marine water input (thick carbonate silty fine sandy succession). Considering the chronostratigraphy of the core and the sea level of the area (Stéphan and Goslin 2014), these sediments are most likely Mid-Holocene transgressive prism controlled by the post-glacial sea level rise and, to a lesser extent, by the tide amplitude. A greater carbonate sedimentation around −8 m bsl could be chronologically associated with a sea-level jump identified in Western Europe (Lawrence et al. 2016) and occurring at the beginning of 8 ka cal. BP. A speculative chronological association can be established with the 8.2 ka BP cold event (Alley et al. 1997) despite no paleoclimatic evidence in the stalagmite record of the Caumont cave, located 30 km southward (Bejarano-Arias 2024). As shown in Figure 8, the palaeoestuary of the LSV extends at least up to the Lower Commerce Valley. Due to the rapid inundation of the estuary, the marine water easily penetrated the Commerce Valley, while the maximum possible extension of the right bank of the Seine's minor bed was likely situated further north than today.

The open marine environment of subtidal flat then evolved into a more closed estuarine landscape, taking place from the fifth mlm BCE to the end of the third mlm BCE (ca. 6.8 to 4.3 ka cal. BP). The decrease in hydrodynamics favoured the accumulation of OM (transported or in situ), characterised by a lower water depth. It may also be associated with the rise of piezometric levels of groundwater, which followed the sea level rise during the Holocene. This landscape permitted the development of wetlands, and because of low hydrodynamics, these plants and

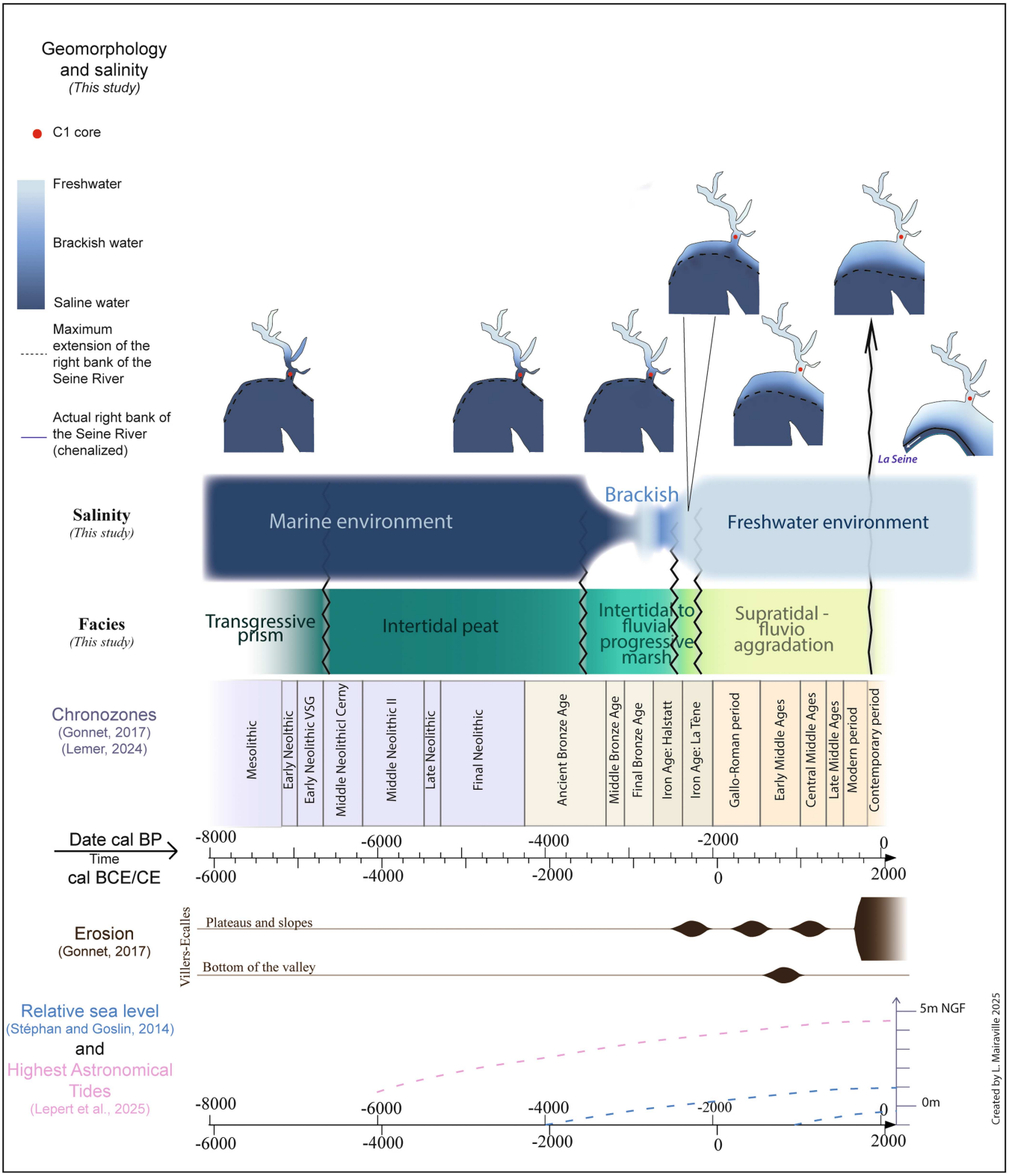

FIGURE 8 | Diachronic evolution model of the Commerce Valley, in contact with the Seine, over the last 6000 years.

OM did not decompose completely due to the lack of oxygen in the water-saturated soil. It accumulated, forming a peaty sediment. The sedimentation rate (0.0693 cm/year, Figure 4) was lower than the underlying sub-facies. The sedimentation here could be interpreted as an aggradation of the right-lateral tidal flat.

The downstream environment of the Commerce Valley then reopened between the end of the third mlm BCE to the middle of the second mlm BCE (ca. 4.1 to 3.6 ka cal. BP) and remained under saline influences as supported by the meso-polyhalobic diatom species (tychoplanktonic species > epontic species). An intrusion of coarser sediments distinguished by alternating

silty-sandy tidal flat and organic layers, thus yielding more OM and favouring mesosaprobic and polysaprobic species. The basis of the lowest encountered environment consists of a transition from outer to inner estuarine tidal flat. During this period (7–3.6 ka cal. BP), the sedimentation rate decreased (Figure 4) and may be related to the slowdown in the relative sea level increase (García-Artola et al. 2018; Stéphan and Goslin 2014) or to the decrease in the accommodation space

Then the marine/estuarine facies (3.6–2.4 ka cal. BP) downstream of the Commerce Valley showed slightly less marine water input in more distal tidal flat areas. It became influenced by freshwater inflows, as shown by oligohalic and oligohalobic-halophilic diatoms and took place for about a millennium. The sedimentation rate for this environment resulted from the combination of fluvial and marine factors with an average of 0.1233 cm/year. The Lower Seine River estuary was still inflowing into the Commerce Valley, but the maximum possible extension of the right bank of the active floodplain of the Seine was gradually shifting southwards (Figure 8), favouring progressive marshes.

From 2.4 to 2 ka cal. BP, the palaeoenvironment exhibited a tipping point from marine to fluvial/continental conditions. Meso-polyhalobic diatom species decreased while oligohalobic and halophilic species increased, showing the salinity of the environment was decreasing, resulting in a brackish environment. The development of mesotrophic and mesosaprobic diatoms suggests a new input of nutrients and OM, probably coming from fluvial sources. This may indicate that the Lower Commerce Valley was no longer marine dominated and influenced by the direct saline tides (probably affecting the water level in the main tidal and fluvial channels), and that the environment progressively changes to a more closed one (Dalrymple and Choi 2007) with more freshwater inputs. The sedimentation rate was around 0.1200 cm/year, which is correlated with the values proposed for the Seine Bay, where Delsinne (2005) demonstrated that prior to 7.5 ka cal. BP, the sedimentation rate was 6.8 mm/year, whereas in the Marais Vernier, it was 5.5 cm/year (Frouin et al. 2007). The downstream part of the Commerce Valley then continued to be filled by sedimentation and became progressively disconnected from the Seine palaeoestuary, as demonstrated by Sechi et al. (2010). The maximum extension of the right bank of the Seine's active floodplain continued shifting southwards, favouring progressive marshes.

Freshwater became predominant from the third century BCE. This area (in the middle of the valley and very close to the actual river) was supratidal, beyond the reach of the highest astronomical tides, as the maximum extension of the north side of the Seine's active floodplain was still aggrading southward. Erosion pressure was increasing on the plateaux and slopes of similar tributary valleys (Gonnet et al. 2023).

From the third century BCE to the middle of the seventh century CE, organic sediment was deposited at a rate of 0.1843 cm/year. These sediments allowed the development of mesotrophic species, although the number of mesosaprobic species was gradually decreasing. This suggests a stabilisation of the local environment, such as a swampy area in the floodplain, with low hydrodynamic activity, stirring and enriching OM, but which still brings some nutrients.

Since the middle of the seventh century CE, a sediment accumulation coming from slopes and plateau erosion overlays previous facies. Various Holocene erosive episodes have been identified in the LSV, showing a tipping point in the origin of erosion, either linked to climate or to human pressure from the Neolithic period onwards (Gonnet 2017; Gonnet et al. 2023; Sechi-Sapowicz 2012), which is still active today (Charpenay 2024).

At around 150 cal. BP (ca. 1800 CE), the palaeogeography of the Lower Commerce Valley and the Seine Estuary can be followed on historical maps such as the *Carte d'Etat-Major* (Carte de l'Etat-Major), where the right bank of the Seine's active floodplain is shown (Figure 8). Then, from ca. 1850 CE (*ca.* 100 cal. BP), major dyke works were carried out in the LSV, resulting in the complete sedimentary disconnection of the Lower Commerce Valley from the main estuary system (Foussard et al. 2010).

5.2 | Implication for the Roman City of *Juliobona*

The results and interpretations proposed here provide a palaeoenvironmental framework for contextualising the local history in Antiquity, using a multiproxy geoarchaeological approach (Figure 9).

The city was founded between the end of the first century BCE and the beginning of the first century CE, under the reign of Augustus, in a freshwater-dominated environment (Figure 9). According to archaeologists (Duval 1984; Fichet de Clairfontaine et al. 2004; Spiesser 2021) the heyday of *Juliobona* is dated to the first and second centuries CE before major changes affected the city in the second half of the third century: reduction of the urban area from 23 to a few hectares, construction of a *castrum*, and territorial regrouping and transfer of the civitas-capital from *Juliobona* to *Rotomagus*, now Rouen (Parétias 2024, 22–26). According to our reconstruction (Section 5.1), the environment does not change during this period.

We demonstrate that during these three periods (foundation, heyday and decline of the city) the Commerce River had freshwater conditions (Figure 9), contradicting previous hypotheses (Duval 1984; Fichet de Clairfontaine et al. 2004), which suggested an environmental change between the beginning of the first and the third centuries CE.

According to archaeological excavations in Lillebonne, no data have been able to establish the existence of a port nor the corollary structure of port activities (quays or even perishable structures) whose filling would explain the major changes that the capital had undergone since the third century CE. Although economic and port activities seem to be attested by Strabo (Strabon, Geographie, IV, 1, 14), the question of the port has been debated for over a century (partial selection: Yvart 1966; Mouchard 2008; Kliesch 2011; Spiesser 2020; Robert 2022) in the absence of tangible evidence (Parétias 2024, 43–44).

Even for the 13th century, studies on the medieval period keep the question of the port unresolved (Dubois 2024): in early literature, the terms 'harbour' (in the meaning of 'haven') and 'quay' appear to have the same meaning in the Lower Commerce Valley. Notably, the word 'port' is conspicuously absent from these texts. When the term 'quays' is employed, it seems to denote structures that were particularly dependent to environmental factors such as sandbanks. This suggests that these quays might have been constructed from perishable materials,

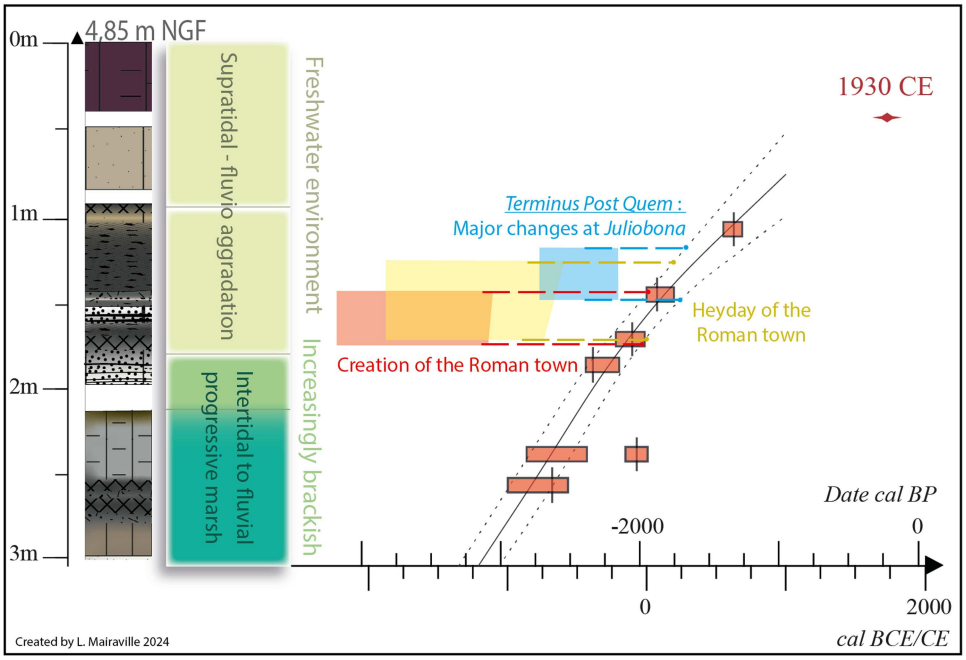

FIGURE 9 | Correlation between key dates in the history of *Juliobona* C1 core and its palaeoenvironmental interpretation.

requiring minimal human effort and thus serving merely as opportunistic points for unloading goods (see Dubois 2024 for sources).

Furthermore, this evidence suggests that unloading activities would not occur along the Commerce River and would therefore take place in the downstream section of the river, at Mesnil-sous-Lillebonne, 1.3 km downstream from Lillebonne's town centre. Then, the hypothesis that a port existed in the Middle Ages as a successor to the Roman port of Lillebonne is unsupported by the current knowledge (Parétias 2024, 43–44). Given the absence of evidence for a port (and not a harbour) near (or at) Lillebonne in the Middle Ages, the question then arises of the existence of a port in Roman times.

Currently, robust environmental evidence solely supports freshwater conditions in the LSV during Antiquity. Therefore, it seemed relevant to investigate the tidal palaeoestuarine system and the presence of a channel, whether anthropogenic or natural, near which correlative structures of port activities could have been installed. However, LiDAR surveys conducted on the site did not reveal any palaeochannels. This could be explained either by a small river-migration over time, by excessive subsequent silting or due to channels that are fossilised or have been rendered invisible for taphonomic reasons.

By way of example, with regard to navigability (or naval competence) and Roman draughts, the Fiumicino 1, 2 and 3 shipwrecks, dating from the fourth and fifth centuries CE, are fluvio-maritime and have a shallow draught between 1.14 and 1.57 m (Boetto 2010). Thus, using regressive reasoning, this kind of boat could have navigated a shallow channel.

Finally, it is essential to discuss the tidal influence during Roman times. In fact, the tidal influence could still have reached *Juliobona* in a freshwater environment, insofar it is necessary to differentiate saline tide (with saline intrusion) from dynamic tide (Savenije 2005), the latter's influence being felt further upstream in the Commerce River. Even in the absence of direct access to the Seine estuary, the area might have been subject to tidal fluctuations. Similar to the port of Irun (Spain) (Urteaga 2020), where boats could ascend the channel by riding the tide twice a day.

All these questions require further geoarchaeological investigations, as a single sediment core is insufficient to answer these spatial inquiries and palaeogeographical reconstructions. New research is necessary, including a sedimentary transect of the Commerce Valley combined with a multiproxy approach to reconstruct tidal environments for ancient periods in relation to human occupations. In order to discuss the presence (or not) of the Roman port, it will be a larger discussion with specialists of archives, *instrumentum*, historiography and archaeological data, for example.

6 | Conclusion

The sedimentary history of the Lower Commerce Valley can be divided into three main periods (Figure 3). The Commerce Valley was incised during the Pleistocene with a glacial-eustatic drop and subsequently clogged due to the post-glacial sea level rise, especially during the early Holocene. The available evidence indicates that the Lower Commerce Valley was initially characterised by open marine facies, where tidal influences were significant before 3.6 ka cal. BP. The marine environment persisted, albeit with a stability reduction (between 3.6 and 2.4 ka cal. BP) over time, with tidal flats migrating during the sedimentary aggradation throughout the Holocene.

The marine/tidal influence then decreased due to the aggradation of tidal flats, as suggested by the decrease in marine flora. However, tidal and alluvial channels still persisted as the environment was dominated by tides, with the growing influence of the Commerce River making the environment increasingly brackish (between 2.4 and 2 ka cal. BP). From a sedimentary point of view, the disconnection of marine

influence (aggradation of the area) then continued slowly until a tipping point during the third century BCE, where the Lower Commerce Valley was strictly under fluvial influence.

The results, complemented by further geomorphological investigations and comparisons with sequence stratigraphy data (McLaughlin 2005), will allow the comparison of the Commerce Valley with other European estuaries, whether clogged or not, and to define its specific features.

As far as the Roman period is concerned, the data provided by core C1 does not allow any definitive conclusions to be drawn about the nature of the sedimentation in the lower part of the Commerce. However, the new evidence suggests a gradual environmental change, rather than a rapid one. In any case, our geoarchaeological results must be treated with caution, and the relevance of core C1 must be confirmed by further work (new cores and geophysical surveys), comparing them with information from archaeological excavations and a multidisciplinary approach. Further investigations are also underway upstream of the Seine, in the Caudebec-en-Caux area (Rives-en-Seine), in order to investigate palaeoenvironmental changes during the Holocene.

Author Contributions

L. Mairaville: conceptualisation, methodology, validation, formal analysis, investigation, resources, writing – original draft, writing – review and editing, visualisation, supervision, project administration, funding acquisition. **S. Chapkanski:** methodology, validation, formal analysis, writing – review and editing, supervision, project administration, funding acquisition. **D. Todisco:** conceptualisation, writing – review and editing, supervision, project administration, funding acquisition. **C. Finco:** methodology, validation, formal analysis, investigation, writing – review and editing. **C. Paillès:** methodology, validation, formal analysis, investigation, writing – review and editing. **J. Parétias:** writing – review and editing, supervision, funding acquisition. **T. Lepert:** conceptualisation, writing – review and editing, supervision. **A. Haddad:** investigation, writing – review and editing. **J. Ducastel:** Formal analysis, methodology, resources, validation, writing – review and editing. **F. Boufflers:** formal analysis, methodology, resources, validation, writing – review and editing. **J. Leleu:** methodology, validation, formal analysis, investigation, writing – review and editing. **L. Dezileau:** methodology, validation, formal analysis. writing – review and editing. **D. Mouralis:** conceptualisation, writing – review and editing, supervision, project administration, funding acquisition.

Acknowledgements

This study was funded by the University of Rouen Normandie and the *Projet Collectif de Recherche Juliobona*. We are grateful to *Caux Seine agglo, Mairie de Lillebonne and SRA Normandie* for their permission and support in providing access to the research sites. We thank all the students and colleagues who helped during fieldwork: Robert Davidson, Mohamed Kouah, Ingrid Bejarano-Arias, Kim Genuite, Igor Girault, from UMR 6266 and Faycal Rejiba from UMR 6143. We would also like to thank Marie-Paule Bataillé for her assistance with the laboratory analyses. Finally, a very big thank you to Lola Bricout, Clément Gouret, Manon Charpenay and all the volunteers who love their region, especially Serge Lejeune and Stéphane Lejeune for their invaluable help during the fieldwork. We express our gratitude to Laboratory Archeorient for the geochemical analysis. A warm thanks to our colleagues (Anne Bocquet-Lienard, Juliette Dupré) from the UMR 6273 for letting us access ICP. A special thanks to Hervé Richard (Chrono-Environnement, UMR 6249), who studied pollen. Thank you to Guillaume Lepert and Maureen Le Doaré for their help with the translation. We are grateful to our colleagues in UMR 6266- IDEES Rouen (Zoé Sicard-Delage, Ingrid Bejarano-Arias and Louisette Garçin) for their help with maps, DEM, reviewing, translation and statistics. The authors are grateful to the two anonymous reviewers for their insightful feedback, which significantly improved earlier versions of the manuscript. We also extend our thanks to the journal's editorial team for their clear communication and meticulous handling of the editorial process. This work was supported by the Universite de Rouen and Caux Seine agglo. Open access publication funding provided by COUPERIN CY26.

Conflicts of Interest

The authors declare no conflicts of interest.

Data Availability Statement

All the data that support the findings of this study are available from the corresponding author upon reasonable request.

References

Antique Source:

Strabon. Géographie. Livres III et IV (vol. 1-17; traduit par F. Lasserre). Les belles lettres.

Source

Allen, P., D. Bain, D. Bridgland, et al. 2022. "Mid-Late Quaternary Fluvial Archives Near the Margin of the MIS 12 Glaciation in Southern East Anglia, UK: Amalgamation of Multi-Disciplinary and Citizen-Science Data Sources." *Quaternary* 5, no. 3: 37. https://doi.org/10.3390/quat5030037.

Alley, R. B., P. A. Mayewski, T. Sowers, M. Stuiver, K. C. Taylor, and P. U. Clark. 1997. "Holocene Climatic Instability: A Prominent, Widespread Event 8200 Yr Ago." *Geology* 25, no. 6: 483. https://doi.org/10.1130/0091-7613(1997)025<0483:HCIAPW>2.3.CO;2.

Antoine, P. 2002. "Les lœss en France et dans le Nord-Ouest européen." *Revue Française de Géotechnique* 99: 3–21. https://doi.org/10.1051/geotech/2002099003.

Antoine, P., S. Coutard, J. J. Bahain, J. L. Locht, D. Hérisson, and E. Goval. 2021. "The Last 750 Ka in Loess–Palaeosol Sequences From Northern France: Environmental Background and Dating of the Western European Palaeolithic." *Journal of Quaternary Science* 36, no. 8: 1293–1310. https://doi.org/10.1002/jqs.3281.

Avoine, J. 1984. "Rapport V.1 L'aménagement de l'estuaire de la Seine. Conséquences sédimentologiques." In *L'hydraulique et la maitrise du littoral. Problèmes côtiers posés par le mouvement des sédiments et la pollution*. Marseille.

Baize, D. 2021. *Guide des analyses en pédologie*. 3ème. Savoir-faire. Editions Quae.

Baize, D., and M.-C. Girard. 2009. *Référentiel pédologique 2008*. Quae.

Baltzer, A., S. Cassen, A.-V. Walter-Simonnet, H. Clouet, A. Lorin, and B. Tessier. 2015. "Variations du niveau marin Holocéne en Baie de Quiberon (Bretagne sud): marqueurs archéologiques et sédimentologiques." In *Quaternaire. Revue de l'Association française pour l'étude du Quaternaire*, 105–115. https://doi.org/10.4000/quaternaire.7201.

Bejarano-Arias, I. 2024. *High Resolution Past Climate and Paleoenvironmental Reconstruction During the Holocene: A Stalagmite-based Records Study From Caumont Cave, Normandy (France)*. Université de Rouen Normandie.

Blanchet, C. L., N. Thouveny, L. Vidal, et al. 2007. "Terrigenous Input Response to Glacial/Interglacial Climatic Variations Over Southern Baja California: A Rock Magnetic Approach." *Quaternary Science Reviews* 26, no. 25/28: 3118–3133. https://doi.org/10.1016/j.quascirev.2007.07.008.

Boetto, G. 2010. "Les navires de Fiumicino: influences fluviales et maritimes." *Publications de l'Institut Français d'Études Anatoliennes* 20, no. 1: 137–150.

Brown, A. G., L. S. Basell, P. S. Toms, J. A. Bennett, R. T. Hosfield, and R. C. Scrivener. 2010. "Later Pleistocene Evolution of the Exe Valley: A Chronstratigraphic Model of Terrace Formation and Its Implications for Palaeolithic Archaeology." *Quaternary Science Reviews* 29, no. 7: 897–912. https://doi.org/10.1016/j.quascirev.2009.12.007.

Canellas, C., A. L. Gibelin, P. Lassègues, M. Kerdoncuff, P. Dandin, and P. Simon. 2014. "Les normales climatiques spatialisées Aurelhy 1981-2010: températures et précipitations." *La Météorologie* 8, no. 85: 47. https://doi.org/10.4267/2042/53750.

Chapkanski, S., K. Jacq, G. Brocard, et al. 2022. "Calibration of Short-Wave InfraRed (SWIR) Hyperspectral Imaging Using Diffuse Reflectance Infrared Fourier Transform Spectroscopy (DRIFTS) to Obtain Continuous Logging of Mineral Abundances Along Sediment Cores." *Sedimentary Geology* 428: 106062. https://doi.org/10.1016/j.sedgeo.2021.106062.

Charpenay, M. 2024. "Étude du processus d'érosion par ruissellement en basse vallée de Seine: quantification spatio temporelle à l'échelle du bassin versant de la rivière du Commerce, analyses comparatives in situ." Mémoire de Master 2, Université de Rennes.

Conyers, L. B., E. G. Ernenwein, M. Grealy, and K. M. Lowe. 2008. "Electromagnetic Conductivity Mapping for Site Prediction in Meandering River Floodplains." *Archaeological Prospection* 15, no. 2: 81–91. https://doi.org/10.1002/arp.326.

Croudace, I. W., and R. G. Rothwell. 2015. "Twenty Years of XRF Core Scanning Marine Sediments: What Do Geochemical Proxies Tell Us?" In *Micro-XRF Studies of Sediment Cores: Applications of a Non-Destructive Tool for the Environmental Sciences. Vol. 17, Developments in Paleoenvironmental Research*. Springer Netherlands.

Cuvilliez, A. 2008. *Dynamiques morphologique et sédimentaire d'une slikke et d'un schorre dans un estuaire macrotidal anthropisé (Seine-France)*. Université de Rouen.

Dalrymple, R. W., and K. Choi. 2007. "Morphologic and Facies Trends Through the Fluvial–Marine Transition in Tide-Dominated Depositional Systems: A Schematic Framework for Environmental and Sequence-Stratigraphic Interpretation." *Earth-Science Reviews* 81, no. 3/4: 135–174. https://doi.org/10.1016/j.earscirev.2006.10.002.

Dalrymple, R. W., B. A. Zaitlin, and R. Boyd. 1992. "Estuarine Facies Models; Conceptual Basis and Stratigraphic Implications." *Journal of Sedimentary Research* 62, no. 6: 1130–1146. https://doi.org/10.1306/D4267A69-2B26-11D7-8648000102C1865D.

David, P.-Y., B. Meire, D. Pennequin, and N. Jallais. 2020. *Fonctionnement de l'hydro-système, interactions et cheminements des eaux naturelles et de la n-nitrosomorpholine dans le secteur de la Faille de Lillebonne – Fécamp (76) – Volet hydrogéologique Rapport final*. BRGM/RP-69139-FR.

Delsinne, N. 2005. *Évolution pluri-millénaire à pluri-annuelledu prisme sédimentaire d'embouchure de la Seine. Facteurs de contrôle naturels et d'origine anthropique*. Université de Caen.

Denys, L. 1991. "A Check-List of the Diatoms in the Holocene Deposits of the Western Belgian Coastal Plain With a Survey of Their Apparent Ecological Requirements. I. Introduction, Ecological Code and Complete List." *Service Géologique de Belgique-Professional paper* 246, no. 2: 1–41.

Dictionary Cambridge. 2025. "Harbour." https://dictionary.cambridge.org/fr/dictionnaire/anglais/harbour.

Dubois, A. 2024. "La disparition du port de Lillebonne (fin du Moyen Âge - époque moderne)." In Parétias, J. 2024. *Rapport d'opération du Projet Collectif de Recherche 2022-2023 «Juliobona, capitale des Calètes»*. https://hal.science/hal-04678191v1.

Duval, P. C. 1984. "Rouen et les voies antiques de Haute-Normandie." *Annales de Normandie* 34, no. 1: 3–13. https://doi.org/10.3406/annor.1984.6378.

Farr, R. H., G. Momber, J. Satchell, and N. C. Flemming. 2017. "Paleolandscapes of the Celtic Sea and the Channel/La Manche." In *Submerged Landscapes of the European Continental Shelf*, edited by N. C. Flemming, J. Harff, D. Moura, A. Burgess and G. N Bailey, 211–239. Wiley.

Fichet de Clairfontaine, F., E. Delaval, V. Hincker, and J. L. Maho. 2004. "Capitales déchues de la Normandie antique. État de la question." *Supplément à la Revue archéologique du centre de la France* 25, no. 1: 141–155.

Foussard, V., A. Cuvilliez, P. Fajon, C. Fisson, P. Lesueur, and O. Macur. 2010. *Evolution morphologique d'un estuaire anthropisé de 1800 à nos jours*. GIP Seine-Aval. https://www.seine-aval.fr/wp-content/uploads/2010/03/2-3-Am%C3%A9nagements.pdf.

Frouin, M. 2007. *Enregistrement sédimentaire des facteurs de contrôle (globaux, régionaux et locaux) sur l'évolution holocène des géosystèmes du Marais Vernier et de la Basse Vallée de Seine dans le cadre de l'Europe du NW*. Université de Rouen.

Frouin, M., A. Durand, D. Sebag, et al. 2009. "Holocene Evolution of a Wetland in the Lower Seine Valley, Marais Vernier, France." *Holocene* 19, no. 5: 717–727. https://doi.org/10.1177/0959683609105295.

Frouin, M., D. Sebag, A. Durand, et al. 2007. "Influence of Paleotopography, Base Level and Sedimentation Rate on Estuarine System Response to the Holocene Sea-Level Rise: The Example of the Marais Vernier, Seine Estuary, France." *Sedimentary Geology* 200, no. 1: 15–29. https://doi.org/10.1016/j.sedgeo.2007.02.007.

García-Artola, A., P. Stéphan, A. Cearreta, R. E. Kopp, N. S. Khan, and B. P. Horton. 2018. "Holocene Sea-Level Database From the Atlantic Coast of Europe." *Quaternary Science Reviews* 196: 177–192. https://doi.org/10.1016/j.quascirev.2018.07.031.

Genuite, K., D. Todisco, C. Nehme, D. Ballesteros, and D. Mouralis. 2021. "Morphological Evolution of the Middle and Lower Seine Valley (Normandy, France) During the Quaternary: Morphometric Analysis of the Paleomeanders." *Quaternaire* 32/3: 203–220. https://doi.org/10.4000/quaternaire.15902.

Genuite, K., P. Voinchet, C. Nehme, et al. 2025. "Quaternary Landscape Evolution of the River Seine (France): Synthesis and New Results From ESR Dating and Magnetostratigraphy of Fluvial and Cave Deposits." *Quaternary Science Reviews* 349: 109063. https://doi.org/10.1016/j.quascirev.2024.109063.

GIP Seine-Aval. 2013. *Contextes climatique, morphologique & hydro-sédimentaire: La salinité dans l'estuaire de la Seine*.

Gonnet, A. 2017. *Du plateau au fond de vallée: apport de l'étude de trois sites archéologiques à la compréhension des dynamiques géomorphologiques holocènes en Normandie*. Université de Rouen Normandie.

Gonnet, A., D. Todisco, M. Rasse, D. Mouralis, and T. Lepert. 2023. "Soil Erosion and Anthropogenic Impact on Landscape Evolution over the Past 2500 Years: A Case Study of the Villers-Ecalles Dry Valley (Seine-Maritime, Normandy, France)." *Geomorphology* 427: 108623. https://doi.org/10.1016/j.geomorph.2023.108623.

Guiry, M. D., and G. M. Guiry. 2025. "AlgaeBase. World-Wide Electronic Publication, University of Galway." https://www.algaebase.org/.

Hammer, O., A. T. H. David, and P. D. Ryan. 2001. "PAST: Paleontological Statistics Software Package for Education and Data Analysis." *Palaeontologia Electronica* 4, no. 1: 4:9.

Havelock, G. M. 2009. "Palaeosalinity Change in the Taw Estuary, South-West England: Response to Late Holocene River Discharge and Relative Sea-Level Change." Ph.D. thesis, University of Exeter (United Kingdom).

Himmelsbach, I., R. Glaser, J. Schoenbein, D. Riemann, and B. Martin. 2015. "Reconstruction of Flood Events Based on Documentary Data and Transnational Flood Risk Analysis of the Upper Rhine and Its French and German Tributaries Since AD 1480." *Hydrology and Earth System Sciences* 19, no. 10: 4149–4164. https://doi.org/10.5194/hess-19-4149-2015.

Holliday, V. T. 1987. "Geoarchaeology and Late Quaternary Geomorphology of the Middle South Platte River, Northeastern Colorado." *Geoarchaeology* 2, no. 4: 317–329. https://doi.org/10.1002/gea.3340020404.

Jaouen, F. 2019. *Ouvrir les paysages de la vallée du Commerce et de ses rivières - Archéologie et prospective entre plateau de Caux et estuaire fossile*. ENSP - AURH.

Khan, N. S., C. H. Vane, B. P. Horton, C. Hillier, J. B. Riding, and C. P. Kendrick. 2015. "The Application of δ13C, TOC and C/N Geochemistry to Reconstruct Holocene Relative Sea Levels and Paleoenvironments in the Thames Estuary, UK." *Journal of Quaternary Science* 30, no. 5: 417–433. https://doi.org/10.1002/jqs.2784.

Kliesch, F. 2011. *Lillebonne, rue de la République (parcelles B143, 144 et BR 33). La nécropole principale de Juliobona, son mur de berge et ses aménagements de rive*.

Knox, J. C. 2006. "Floodplain Sedimentation in the Upper Mississippi Valley: Natural Versus Human Accelerated." *Geomorphology* 79, no. 3: 286–310. https://doi.org/10.1016/j.geomorph.2006.06.031.

Laignel, B., F. Quesnel, R. Meyer, and P. Lebret. 1998. "Les biefs a silex; depots periglaciaires de versant issues des alterites a silex de plateau du bassin de Paris." *Bulletin de la Société Géologique de France* 169, no. 4: 605–612.

Lamb, A. L., C. H. Vane, G. P. Wilson, J. G. Rees, and V. L. Moss-Hayes. 2007. "Assessing δ13C and C/N Ratios From Organic Material in Archived Cores as Holocene Sea Level and Palaeoenvironmental Indicators in the Humber Estuary, UK." *Marine Geology* 244, no. 1: 109–128. https://doi.org/10.1016/j.margeo.2007.06.012.

Lange-Bertalot, H., M. W. G. Hofmann, M. Kelly, and M. Cantonati. 2017. *Freshwater Benthic Diatoms of Central Europe: Over 800 Common Species Used in Ecological Assessment*. Vol. 942. Koeltz Botanical Books.

Langevin, C. 1998. *Vallée du Commerce (Seine-Maritime) - Relations nappe/rivière. Etude bibliographique et synthèse*. BRGM R 40 488.

Lawrence, T., A. J. Long, W. R. Gehrels, L. P. Jackson, and D. E. Smith. 2016. "Relative Sea-Level Data From Southwest Scotland Constrain Meltwater-Driven Sea-Level Jumps Prior to the 8.2 kyr BP Event." *Quaternary Science Reviews* 151: 292–308. https://doi.org/10.1016/j.quascirev.2016.06.013.

Ledieu, L., A. Simonneau, O. Cerdan, et al. 2020. "Geochemical Insights Into Spatial and Temporal Evolution of Sediment at Catchment Scale (Egoutier Stream, France)." *Applied Geochemistry* 122: 104743. https://doi.org/10.1016/j.apgeochem.2020.104743.

Lemoine, J.-P. 2021 *Dynamique morpho-sédimentaire de l'estuaire de la Seine: rôle des dragages d'entretien*. Université de Bretagne occidentale.

Lespez, L. 2025. "Environmental Determinism: A Critical Perspective and New Approaches to Understanding the Relationship Between Pre- and Protohistoric Societies and Their Environment." *Bulletin de la Société préhistorique française*.

Lesueur, P., S. Lesourd, D. Lefebvre, S. Garnaud, and J. C. Brun-Cottan. 2003. "Holocene and Modern Sediments in the Seine Estuary (France): A Synthesis." *Journal of Quaternary Science* 18, no. 3/4: 339–349. https://doi.org/10.1002/jqs.755.

Long, A. J., R. G. Scaife, and R. J. Edwards. 2000. *Stratigraphic Architecture, Relative Sea-Level, and Models of Estuary Development in Southern England: New Data From Southampton Water*, Vol. 175, 253–279. Special Publications. https://doi.org/10.1144/GSL.SP.2000.175.01.19.

Łukowiak, M. 2020. "Utilizing Sponge Spicules in Taxonomic, Ecological and Environmental Reconstructions: A Review." *PeerJ* 8: e10601. https://doi.org/10.7717/peerj.10601.

Mairaville, L., S. Chapkanski, and D. Todisco, et al. 2024a. *Évolution environnementale holocène dans l'estuaire de la Seine: Juliobona et la vallée du Bolbec/Commerce*. Actes du 3ème Colloque de l'APVSM.

Mairaville, L., S. Chapkanski, and D. Todisco, et al. 2024b. *Géoarchéologie et géomorphologie de la basse vallée du Commerce (résultats 2022 – 2023)*, 77–110.

McLaughlin, P. P. 2005. "Sequence Stratigraphy." In *Encyclopedia of Geology*, 159–173. Elsevier. https://doi.org/10.1016/B0-12-369396-9/00043-5.

Meire, B., A. Portal, and T. Jacob, et al. 2019. *Fonctionnement de l'hydrosystème, interactions et cheminements des eaux naturelles et de la n-nitrosomorpholine dans le secteur de la Faille de Lillebonne – Fécamp (76) – Volet géologique et géophysique Rapport final*. BRGM/RP-67087-FR.

Menillet, F. 1969. *Notice explicative Bolbec*. Carte géologique France (1/50000), feuille Bolbec BRGM.

Mertens, A., J. van der Wal, G. Verweij, B. Pex, A. Van Dulmen, and H. Van Dam. 2025. "A Revised List of Diatom Ecological Indicator Values in The Netherlands." *Ecological Indicators* 172: 113219. https://doi.org/10.1016/j.ecolind.2025.113219.

MétéoFrance. n.d. "Carte des cumuls de précipitations quotidiennes. Normales calculées sur 1971–2000."

Mouchard, J. 2008. "De la voie navigable aux sites portuaires en basse vallée de Seine: maîtrise et gestion des accès (Antiquité - époque moderne)." In *Des châteaux et des sources: Archéologie et histoire dans la Normandie médiévale, Hors collection*, edited by J.-L. Roch, B. Lepeuple, and É. Lalou, 103–127. Presses universitaires de Rouen et du Havre. https://doi.org/10.4000/books.purh.9975.

Nanson, R., R. Arosio, and J. Gafeira, et al. 2023. *A Two-Part Seabed Geomorphology Classification Scheme; Part 2: Geomorphology Classification Framework and Glossary (Version 1.0)*. Zenodo. https://doi.org/10.5281/ZENODO.7804019.

Notebaert, B., and G. Verstraeten. 2010. "Sensitivity of West and Central European River Systems to Environmental Changes During the Holocene: A Review." *Earth-Science Reviews* 103, no. 3: 163–182. https://doi.org/10.1016/j.earscirev.2010.09.009.

Orth, P., A. G. Jean François Pastre, N. Limondin-Lozouet, and S. Kunesch. 2004. "Les enregistrements morphosédimentaires et biostratigraphiques des fonds de vallée du bassin-versant de la Beuvronne (Bassin parisien, Seine-et-Marne, France): perception des changements climatoanthropiques à l'Holocène [Holocene Morpho-Sedimentary and Bio-Stratigraphy Records From Alluvial Fills of the Beuvronne River Catchment (Paris Basin, France): Perception of Climatic Changes and Human Activities]." *Quaternaire* 15, no. 3: 285–298. https://doi.org/10.3406/quate.2004.1775.

Parétias, J. 2024. *Projet Collectif de Recherche « Juliobona, capitale des Calètes » Rapport d'opération 2022–2023*. https://hal.science/hal-04678191v1.

Parfitt, S. A., N. M. Ashton, S. G. Lewis, et al. 2010. "Early Pleistocene Human Occupation at the Edge of the Boreal Zone in Northwest Europe." *Nature* 466, no. 7303: 229–233. https://doi.org/10.1038/nature09117.

Peet, R. K. 1974. "The Measurement of Species Diversity." *Annual Review of Ecology and Systematics* 5: 285–307.

Pribyl, D. W. 2010. "A Critical Review of the Conventional SOC to SOM Conversion Factor." *Geoderma* 156, no. 3/4: 75–83. https://doi.org/10.1016/j.geoderma.2010.02.003.

Quesnel, F. 1997. *Cartographie numérique en géologie de surface. Application aux altérites à silex de l'Ouest du bassin de Paris*. Université de Rouen.

Reimer, P. J., W. E. N. Austin, E. Bard, et al. 2020. "The IntCal20 Northern Hemisphere Radiocarbon Age Calibration Curve (0–55 Cal kBP." *Radiocarbon* 62, no. 4: 725–757. https://doi.org/10.1017/RDC.2020.41.

Robert, M. 2022. *L'instrumentum d'époque romaine dans l'estuaire de la Seine*. Nantes Université.

Rothwell, R. G., B. Hoogakker, J. Thomson, I. W. Croudace, and M. Frenz. 2006. "Turbidite Emplacement on the Southern Balearic Abyssal Plain (Western Mediterranean Sea) During Marine Isotope Stages 1–3: An Application of ITRAX XRF Scanning of Sediment Cores to Lithostratigraphic Analysis." *Geological Society, London, Special Publications* 267, no. 1: 79–98. https://doi.org/10.1144/GSL.SP.2006.267.01.06.

Samouëlian, A., I. Cousin, A. Tabbagh, A. Bruand, and G. Richard. 2005. "Electrical Resistivity Survey in Soil Science: A Review." *Soil and Tillage Research* 83, no. 2: 173–193. https://doi.org/10.1016/j.still.2004.10.004.

Savenije, H. H. G. 2005. *Salinity and Tides in Alluvial Estuaries*, 1st ed. Elsevier.

Schrader, H. 1974. "Proposal for a Standardized Method of Cleaning Diatom-Bearing Deep-Sea and Land-Exposed Marine Sediments." *Nova Hedwigia Beihefte* 45: 403–409.

Sebag, D. 2002. *Apports de la matière organique pour la reconstitution des paleoenvironnements holocenes de la basse vallée de la Seine - Fluctuations des conditions hydrologiques locales et environnements de dépôt*. Université de Rouen.

Sechi, S., D. Sebag, B. Laignel, T. Lepert, M. Frouin, and A. Durand. 2010. "Histoire de la sédimentation détritique des derniers millénaires dans la basse vallée de la Seine." In *Journées archéologiques de Haute-Normandie*, edited by A. Bourdon. Presses universitaires de Rouen et du Havre. https://doi.org/10.4000/books.purh.6899.

Sechi-Sapowicz, S. 2012. *Les archives sédimentaires témoins des phases d'érosion - Approche géo-archéologique appliquée au bassin versant de la Basse Vallée de la Seine (Normandie, France) et au Campidano Septentrional (Sardaigne, Italie)*. Université de Rouen.

Shannon, C. E., and W. Weaver, 1948. *The Mathematical Theory of Communication*. Univ. Illinois Press.

Shirzaditabar, F., and R. J. Heck. 2022. "Characterization of Soil Magnetic Susceptibility: A Review of Fundamental Concepts, Instrumentation, and Applications." *Canadian Journal of Soil Science* 102, no. 2: 231–251. https://doi.org/10.1139/cjss-2021-0040.

Sorrel, P., B. Tessier, F. Demory, N. Delsinne, and D. Mouazé. 2009. "Evidence for Millennial-Scale Climatic Events in the Sedimentary Infilling of a Macrotidal Estuarine System, the Seine Estuary (NW France)." *Quaternary Science Reviews* 28, no. 5: 499–516. https://doi.org/10.1016/j.quascirev.2008.11.009.

Spiesser, J. 2020. *Lillebonne -Promenade archéologique de la préhistoire au XIX^{e} siècle*. Editions Snoeck.

Spiesser, J. 2021. *PCR CapCal Juliobona, capitale des calètes - Rapport 2021*.

Stéphan, P., and J. Goslin. 2014. "Évolution du niveau marin relatif à l'Holocène le long des côtes françaises de l'Atlantique et de la Manche: réactualisation des données par la méthode des « sea-level index points." *Quaternaire* 25/4: 295–312. https://doi.org/10.4000/quaternaire.7269.

Urteaga, M. 2020. "Les ports romains dans les Trois Gaules." *Gallia* 77, no. 1: 475–488. https://doi.org/10.4000/gallia.5753.

Verger, F. 1995. "Slikkes et Schorres: milieux et aménagement." *Norois* 165, no. 1: 235–245. https://doi.org/10.3406/noroi.1995.6622.

Verhegge, J., T. Saey, M. Van Meirvenne, T. Missiaen, and P. Crombé. 2017. "Reconstructing Early Neolithic Paleogeography: EMI-Based Subsurface Modeling and Chronological Modeling of Holocene Peat below the Lower Scheldt Floodplain in NW Belgium." *Geoarchaeology* 32, no. 2: 159–176. 76. https://doi.org/10.1002/gea.21581.

Vos, P. C., and H. de Wolf. 1993. "Diatoms as a Tool for Reconstructing Sedimentary Environments in Coastal Wetlands; Methodological Aspects." *Hydrobiologia* 269–270, no. 1: 285–296. https://doi.org/10.1007/BF00028027.

Witkowski, A., H. Lange-Bertalot, and D. Metzeltin. 2000. *Diatom Flora of Marine Coasts*. Springer. Iconographia Diatomologica. A.R.G. Gantner Verlag.

Yvart, M. 1966. *Essai sur la topographie antique de Lillebonne: "Juliobona, le port du IIe siècle"*. Archive départementale de Seine-Maritime.

Sitography

Site hydrométrique - H322 0110: La Seine à Poses: https://www.hydro.eaufrance.fr/sitehydro/H3220110/fiche.

Site hydrométrique - H513 0610: Le Commerce à Gruchet-le-Valasse: https://www.hydro.eaufrance.fr/stationhydro/H513061010/fiche.

Site hydrométrique - H513 0620: Le Commerce à Lillebonne: https://www.hydro.eaufrance.fr/stationhydro/H513062012/fiche.

Old Maps

Carte de l'Etat-Major, feuille Yvetot-Le Havre, Echelle 1/40000. https://remonterletemps.ign.fr/telecharger/?lon=0.539527&lat=49.521299&z=11&layer=ETATMAJOR.

Carte de l'Etat-Major, feuille Lisieux, Echelle 1/40000. https://remonterletemps.ign.fr/telecharger/?lon=0.539527&lat=49.521299&z=11&layer=ETATMAJOR.

Supporting Information

Additional supporting information can be found online in the Supporting Information section.
Mairaville et al_2025_Geoarch__4_SupInf_Accepted_Changes.